

# Reconnaissance ultracool spectra in the *Euclid* Deep Fields

J.-Y. Zhang<sup>1,2</sup>, N. Lodieu<sup>1,2</sup>, and E. L. Martín<sup>1,2</sup>

<sup>1</sup> Instituto de Astrofísica de Canarias (IAC), Calle Vía Láctea s/n, 38200 La Laguna, Tenerife, Spain  
e-mail: jzhang@iac.es

<sup>2</sup> Departamento de Astrofísica, Universidad de La Laguna (ULL), Avenida Astrofísico Francisco Sánchez s/n, 38206 La Laguna, Tenerife, Spain

April 23, 2024

## ABSTRACT

**Context.** The *Euclid* spacecraft has been launched and will carry out a deep survey benefiting the discovery and characterisation of ultracool dwarfs (UCDs), especially in the *Euclid* Deep Fields (EDFs), which the telescope will scan repeatedly throughout its mission. The photometric and spectroscopic standards in the EDFs are important benchmarks, crucial for the classification and characterisation of new UCD discoveries and for the calibration of the mission itself.

**Aims.** We aim to provide a list of photometric UCD candidates and collect near-infrared reconnaissance spectra for M, L, and T-type UCDs in the EDFs as future *Euclid* UCD references.

**Methods.** In EDF North, we cross-matched public optical and infrared surveys with certain photometric criteria to select UCDs. In EDF Fornax and EDF South, we used photometrically classified samples from the literature. We also include UCDs identified by *Gaia* DR2. We selected seven UCD targets with different spectral types from the lists and obtained low-resolution 0.9–2.5  $\mu\text{m}$  spectra of them using GTC/EMIR and the VLT/X-shooter. We also selected a young, bright L dwarf near EDF Fornax to test the coherence of these two facilities. We included one extra T dwarf in EDF North with its published *J*-band spectrum.

**Results.** We retrieved a list of 81 (49, 231) M, eight (29, 115) L, and one (0, 2) T dwarf candidates in EDF North, Fornax, and South, respectively. They are provided to guide future UCD discoveries and characterisations by *Euclid*. In total, we collected near-infrared spectra for nine UCDs, including two M types, three L types, and four T types in or close to the three EDFs. The Euclidised spectra show consistency in their spectral classification, which demonstrates that slitless *Euclid* spectroscopy will recover the spectral types with high fidelity for UCDs, both in the EDFs and in the wide survey. We also demonstrate that *Euclid* will be able to distinguish different age groups of UCDs.

**Key words.** euclid – ultracool dwarfs – photometric standard – spectroscopic standard

## 1. Introduction

Ultracool dwarfs (UCDs), including the lowest-mass stars, brown dwarfs (BDs), and planetary mass objects (PMOs), are the dimmest, coldest objects among our Galactic population. As the name suggests, these objects can have effective temperatures from 2700 K (Kirkpatrick et al. 1995) down to around 250 K, the lowest known so far (Luhman 2014). The established spectral classes for UCDs are the late-M type (M7 and later, Kirkpatrick et al. 1997), the L type (Martín et al. 1997, 1998, 1999; Kirkpatrick et al. 1999, 2000), the T type (Burgasser et al. 2002; Geballe et al. 2002; Burgasser et al. 2006), and recently the Y type (Delorme et al. 2008; Cushing et al. 2011; Kirkpatrick et al. 2011) with decreasing temperature.

Nowadays, we believe that the census of UCD is still incomplete beyond 20 pc. The coldest population with spectral types later than T8 has not been explored thoroughly even within 20 pc (Kirkpatrick et al. 2021). An appropriate method of discovering a UCD population is a deep, wide survey at the near-infrared (NIR) wavelength (Cushing 2014). This is because UCDs are faint and have their emission peaks in the NIR, and they are scattered all over the sky.

Space telescopes such as the Hubble Space Telescope (HST) and the James Webb Space Telescope (JWST), or space surveys like the *Gaia* mission (*Gaia* Collaboration et al. 2016) and the Wide-field Infrared Survey Explorer (WISE; Wright et al.

2010), have the great advantage of being free of atmospheric influences compared with ground-based facilities. HST has discovered many UCDs in its deep fields (Pirzkal et al. 2005, 2009; Stanway et al. 2008; Ryan et al. 2005, 2011; Holwerda et al. 2014; van Vledder et al. 2016; Aganze et al. 2022a,b). JWST has also discovered many UCDs in several fields of its Early Release Observations (Wang et al. 2023; Nonino et al. 2023; Holwerda et al. 2024) and galactic surveys (Hainline et al. 2023), including a discovery of the farthest BD to date at 4.8 kpc (Langeroodi & Hjorth 2023). JWST also demonstrated its power in characterising UCDs (Beiler et al. 2023; Burgasser et al. 2024; Holwerda et al. 2024; Manjavacas et al. 2024). *Gaia* not only discovers UCDs in the whole sky (Reylé 2018; Sarro et al. 2023) but also performs low-resolution spectroscopy on UCDs (Cooper et al. 2024); its precise astrometry reveals UCD companions of the other stars (Stevenson et al. 2023). WISE has also contributed to UCD discoveries (Kirkpatrick et al. 2011), especially the coldest population (Cushing et al. 2011, 2014), thanks to its specially designed passbands (Wright et al. 2010) and whole-sky coverage. Next-generation space telescopes like the Nancy Grace Roman Space Telescope will offer a great opportunity for UCD sciences as well (Holwerda et al. 2023).

*Euclid*<sup>1</sup> (Laureijs et al. 2011), a 1.2-m space telescope launched on July 1 2023, is a European Space Agency (ESA)

<sup>1</sup> <https://www.cosmos.esa.int/web/euclid>

mission aiming to conduct a deep survey covering  $\approx 14500$  deg<sup>2</sup> of the sky in the coming six years. *Euclid* is equipped with optical and infrared capabilities, with the Visible Instrument (VIS) and the Near Infrared Spectrometer and Photometer (NISP) on board. Compared with HST or JWST, a huge advantage of *Euclid* is its wide field of view (FoV). The VIS has an FoV of  $0.787$  deg  $\times$   $0.709$  deg in the  $I_E$  band; the NISP covers the  $Y_E$ ,  $J_E$ , and  $H_E$  bands and has an FoV of  $0.763$  deg  $\times$   $0.722$  deg. The *Euclid* Wide Surveys (EWSs) will have a  $5\text{-}\sigma$  limit of 26.2 mag, 24.3 mag, 24.5 mag, and 24.4 mag in the  $I_E$ ,  $Y_E$ ,  $J_E$ , and  $H_E$  bands, respectively (Euclid Collaboration et al. 2022b). Compared with Gaia, *Euclid* is much more sensitive to UCDs. *Euclid* has a much better spatial resolution than WISE. The NISP can also perform low-resolution slitless spectroscopy ( $R \approx 380$  for point sources) from  $1.25\text{--}1.85$   $\mu\text{m}$  by the red grism and  $0.92\text{--}1.30$   $\mu\text{m}$  by the blue grism, but only in the EDFs (Euclid Collaboration et al. 2023). The spectroscopy enables the spectral classification of UCDs. *Euclid* will be a powerful tool with which to hunt and characterise undiscovered UCDs (Solano et al. 2021; Martín et al. 2021).

Three EDFs,<sup>2</sup> North, Fornax, and South, are the patches of the sky that *Euclid* will repeatedly scan during its lifetime. They consist of a total of 53 deg<sup>2</sup> of sky. After the co-adding, the depth in these regions will be about two magnitudes deeper than the EWSs. For point sources, it will reach an unprecedented  $5\text{-}\sigma$  limit about 26.3, 26.5, 26.4 mag (AB system) in the  $Y_E$ ,  $J_E$ , and  $H_E$  bands, respectively (Euclid Collaboration et al. 2022b,a, 2023). *Euclid* will unveil UCDs far beyond the Galactic disc. In addition, monthly visits makes precise astrometry possible, which is key to measure parallaxes and proper motions of UCDs. The parallax is indispensable in determining the luminosity of UCDs; the proper motion together with the radial velocity from a coarse spectroscopic measurement can classify the objects into different kinematic groups. The Large Synoptic Survey Telescope (LSST) of the Vera C. Rubin Observatory at Cerro Pachón, Chile will complement *Euclid*'s coverage, especially the two southern EDFs at optical wavelengths in depth. (Rhodes et al. 2017).

*Euclid* has  $Y_E$ ,  $J_E$ ,  $H_E$ -band filters and photometric systems that are different from the NIR systems of ground-based surveys such as the 2MASS, Mauna Kea Observatories (MKO), or the VHS (Euclid Collaboration et al. 2022c). The *Euclid* optical filter is much broader than the  $i$  or  $z$  filters of the PS1 and the DES as well. In addition, the ground-based surveys suffer a lot from telluric attenuation. A correction must be applied to the photometric measurements, if we are to use the ground-based data, before they can serve towards the calibration of *Euclid*. Euclid Collaboration et al. (2022c) presented linear transformations between the *Euclid* NISP photometric system and the other ground-based photometric system for M, L, and T-type UCDs. It fitted the simulated photometry of M, L, and T dwarfs from Euclid Collaboration et al. (2019), who used observational templates to calculate corresponding colours. However, the transformations have great residuals. Therefore, having a list of UCDs characterised in the three EDFs prior to the start of the *Euclid* surveys is important. They serve as photometric and spectroscopic standard anchors before the very first nominal survey observations of *Euclid* and they will help *Euclid* to calibrate itself every time it goes back and points at the EDFs.

In this work, we selected UCD candidates as photometric and spectroscopic standards in the three EDFs: North, Fornax, and South. These photometric standards and reconnais-

sance spectral templates are ready for the first data release of *Euclid*. Section 2 explains the UCD selection. We spectroscopically characterised their representatives using the 10.4-m Gran Telescopio Canarias (GTC) on the Spanish island of La Palma (for EDFs North and Fornax) and the European Southern Observatory (ESO) 8.2-m Very Large Telescope (VLT) on Cerro Paranal, Chile (for EDF South). Section 3 describes the observation details. Section 4 explains the spectral classification method. Section 5 shows the results of spectral analysis for each object, and discusses the capability of *Euclid* in terms of UCD characterisation.

## 2. UCD samples in the EDFs

We used the Tool for OPERations on Catalogues And Tables (TOPCAT; Taylor 2005) to cross-match existing catalogues and select UCD candidates in specific areas. We used different criteria and techniques to make the selection in the three different regions.

### 2.1. *Euclid* Deep Field North

EDF North originally was a 10 deg<sup>2</sup> circled area centered at the coordinate 17h58m55.9s +66°01'03.7" with a radius of 1.78 deg. In April 2022, a request to extend EDF North's area to 20 deg<sup>2</sup> (radius extended to 2.52 deg) was endorsed by ESA based on the need for a larger area of spectroscopic calibration.

We collected information on the  $i$  and  $z$  bands from the Panoramic Survey Telescope and Rapid Response System release 1 (Pan-STARRS, PS1; Chambers et al. 2016),  $J$ ,  $H$ , and  $K$  bands from the Two Micron All Sky Survey (2MASS; Cutri et al. 2003; Skrutskie et al. 2006), and  $W1, 2, 3, 4$  bands from the AllWISE programme (Cutri et al. 2021) of WISE. We cross-matched all the point sources in these three catalogues with a radius of 3 arcsec inside EDF North.

To select the UCDs, we applied photometric criteria from Carnero Rosell et al. (2019), but we generalised and slightly loosened the criteria according to the colours presented in Schmidt et al. (2015); Skrzypek et al. (2016). In practice, for late-M UCDs, we required

- $i - z > 0.65$  mag;
- $2.68 < i - J < 4.0$  mag;
- $1.59 < z - J < 2.55$  mag;
- $z - W1 < 4.5$  mag;
- $J - H > 0.47$  mag;
- $J - W2 > 1.36$  mag;
- $H - K > 0.17$  mag;
- $0.13 < W1 - W2 < 0.25$  mag; and
- $SNR_{W4} \leq 3$ .

The colour criterion,  $W1 - W2 > 0.13$  mag, already separates most of the red giants from the dwarfs (Li et al. 2016). To further ensure that we would not include any possible red giants, which could possess big and cooler envelopes, a non-detection criterion in the  $W4$  was set by limiting the signal-to-noise ratio (SNR) of this band. We found 90 late-M UCDs. We note that in our search we did not classify the objects into subclasses.

Reylé (2018) selected UCDs from *Gaia* DR2 based on the locus of spectroscopically confirmed UCDs in the Hertzsprung–Russel (HR) diagram. There are in total 12 UCDs, all late-M type with tentative spectral classification (eight M7 dwarfs, three M7.5 dwarfs, and one M7 subdwarf) in EDF North. Our search recovered ten of these 12 M dwarfs in the catalogue

<sup>2</sup> <https://www.cosmos.esa.int/web/euclid/euclid-survey>

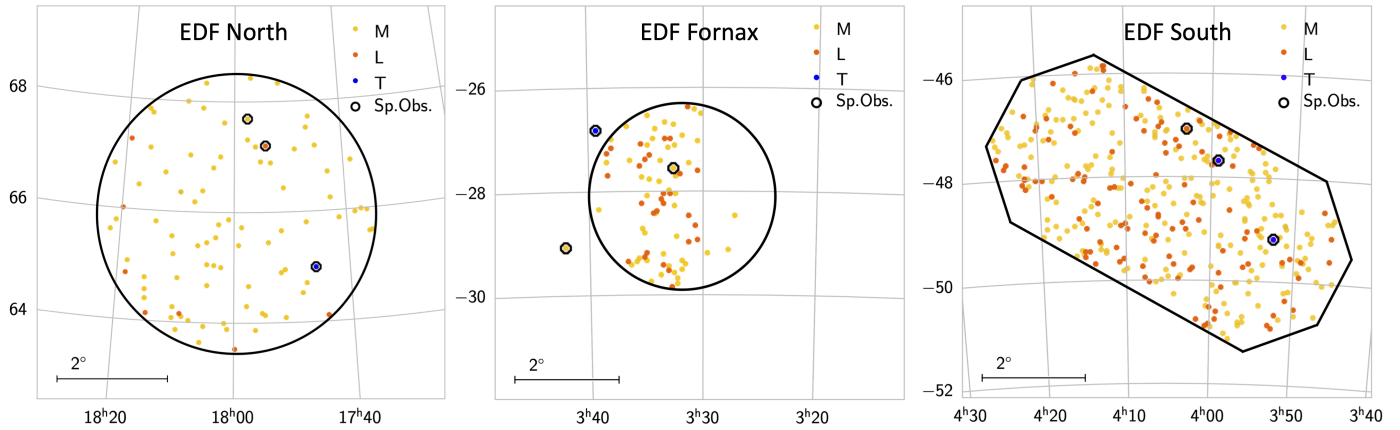


**Fig. 1.** UCD candidates in the three EDFs (black borders). The circled objects are the ones for which we will get spectra.

**Table 1.** Targets selected for spectroscopic observation.

Name	Location	$Y$	$J$	$H$	SpT.	Note
WISEA J175730.71+674138.4	EDF North	15.2	13.7	13.2	<sup>(1)</sup> M7.0	
WISEA J175410.34+671212.0	EDF North	18.0	16.1	15.5	L	Potential binary
<sup>(2)</sup> WISE J174556.65+645933.8	EDF North	-	-	-	T7.0	$J$ band spectrum by (2)
WISEA J033234.35-273333.8	EDF Fornax	18.9	17.2	16.7	M9.0	
<sup>(3)</sup> WISEA J033921.70-264906.5	EDF Fornax*	20.9	18.4	18.7	T6.0	
WISEA J040254.85-470440.9	EDF South	20.9	18.9	-	L5.0	
WISEA J035231.80-491059.4	EDF South	20.3	17.8	18.2	T7.0	
WISEA J035909.75-474056.8	EDF South	20.6	18.1	18.3	T8.0	
<sup>(3)</sup> WISEA J034209.37-290431.9	EDF Fornax*	18.1	15.9	15.1	L4.0, <sup>(6)</sup> L0 $\beta$	GTC & VLT common target

**Note :** In the rest of the paper, we subsequently use *WISEhmm* or *Whhmm*, or *2MASShmm*, as abbreviations. Tables in the appendices provide precise photometry with errors and references.

\*: WISE0339 and WISE0342 are outside but close to the EDF Fornax border, illustrated in the middle panel of Figure 1.

**References.** (1). Reylé (2018); (2). Mace et al. (2013); (3). Carnero Rosell et al. (2019); (4). Burgasser et al. (2015), photometry from the 2MASS; (5). Hsu et al. (2021), photometry from the 2MASS; (6). Gagné et al. (2015).

of Reylé (2018). The other two have a slightly bluer  $J - W2$  colour. We decided to include these two objects. Therefore, we have 81 late-M UCDs in EDF North (Table A.1).

For L-type UCDs, we required redder  $i - z$ ,  $i - J$ ,  $z - J$ , and  $z - W1$  colours (Carnero Rosell et al. 2019):

- $i - z > 1.35$  mag;
- $i - J \geq 4.0$  mag;
- $z - J \geq 2.55$  mag;
- $z - W1 \geq 4.5$  mag;
- $J - H > 0.47$  mag;
- $J - W2 > 1.36$  mag;
- $H - K > 0.17$  mag;
- $W1 - W2 \geq 0.25$  mag;
- $SNR_{W4} \leq 3$ .

We found eight L-type UCDs (Table A.2).

For T dwarfs, because methane absorption starts to play a role in the NIR, the  $J - H$  and  $H - K$  colours turn bluer when the type gets later (Leggett et al. 2003). Hence, we separated the criteria of the early-type and late-type T dwarfs. For early-T-type UCDs, we required

- $z - J > 1.59$  mag;
- $1 < W1 - W2 < 2$  mag;
- $SNR_{W4} \leq 3$ ,

and for late-T-type UCDs, we required

- $J - H < -0.3$  mag;
- $H - K < 0.2$  mag;
- $W1 - W2 > 1.5$  mag; and
- $SNR_{W4} \leq 3$ .

Unfortunately our search found no T dwarf in EDF North. However, we noticed that there is a T7 dwarf WISE J174556.65+645933.8 in EDF North revealed by Mace et al. (2013) in WISE. This object is too faint to be detected by the PS1 or the 2MASS. The  $J$ -band spectrum was already obtained by Mace et al. (2013) using the Near-Infrared Spectrometer (NIRSPEC; McLean et al. 1998, 2000) of the 10-m Keck telescope on Mauna Kea, and was kindly provided to us by Dr. Gregory Mace.

We selected the M dwarf WISE1757 and the L dwarf WISE1754 for spectroscopic characterisation (Table 1). We note that WISE1754 could be an L-dwarf binary system consisting of *Gaia* DR3 1633622185772907392 (hereafter WISE1754 A) and *Gaia* DR3 1633622181475606528 (hereafter WISE1754 B), which were not resolved in WISE and the 2MASS. WISE1754 B is bluer than WISE1754 A. The left panel in Figure 1 shows the UCD candidates in EDF North.

**Table 2.** Summary of GTC/EMIR and VLT/X-shooter observations.

Name	MJD	Seeing	Configuration	Grism/Arm/Filter	Exposures	Std. star
WISE0332	59890.09	0.7"	EMIR Long Slit	<i>YJ</i>	360s×8	τ For
WISE0332	59890.13	0.6"	EMIR Long Slit	<i>HK</i>	240s×12	τ For
WISE0339	59931.95	0.8"	EMIR Long Slit	<i>YJ</i>	360s×8	τ For
WISE0339	59932.93	0.7"	EMIR Long Slit	<i>YJ</i>	360s×8	τ For
WISE0339	59931.99	0.7"	EMIR Long Slit	<i>HK</i>	240s×12	τ For
WISE0339	59932.96	0.8"	EMIR Long Slit	<i>HK</i>	240s×12	τ For
WISE0342	59862.11	0.8"	EMIR Long Slit	<i>YJ</i>	200s×8	HD 20423
WISE0342	59905.12	1.0"	EMIR Long Slit	<i>HK</i>	240s×8	HD 20423
WISE0342	60247.70	2.3"	X-shooter	UVB, VIS, NIR	(276s, 292s, 300s)×8	HD 16226
WISE0352	60246.71	1.4"	X-shooter	UVB, VIS, NIR	(276s, 292s, 300s)×12	HD 207158
WISE0359	60246.76	1.6"	X-shooter	UVB, VIS, NIR	(276s, 292s, 300s)×12	HD 207158
WISE0402	60247.78	3.3"	X-shooter	UVB, VIS, NIR	(276s, 292s, 300s)×12	HD 16226
WISE1754 AB	59831.91	0.7"	EMIR Imaging	<i>J</i>	5s×14	–
WISE1754 AB	59834.98	0.9"	EMIR Long Slit	<i>YJ</i>	320s×8	55 Dra
WISE1754 AB	59835.03	0.8"	EMIR Long Slit	<i>HK</i>	280s×8	55 Dra
WISE1757	59831.93	0.7"	EMIR Long Slit	<i>YJ</i>	120s×8	55 Dra
WISE1757	59831.95	0.7"	EMIR Long Slit	<i>HK</i>	60s×16	55 Dra

**Note:** Candidates are ordered by right ascension. MJD indicates the Modified Julian Date at the middle of each observation.

## 2.2. Euclid Deep Field Fornax

*Euclid* Deep Field Fornax is a 10 deg<sup>2</sup> circled area centered on the coordinate 03h31m43.6s –28°05′18.6″ with a radius of 1.78 deg. Carnero Rosell et al. (2019) did a UCD census in an area about 2400 deg<sup>2</sup>, using the *i*, *z*, and *Y* bands of the Dark Energy Survey (DES; Dark Energy Survey Collaboration et al. 2016) Year 3 release, matched to the *J*, *H*, and *K<sub>s</sub>* bands of the Vista Hemisphere Survey (VHS; McMahon et al. 2013) DR3 and the *W1*, *W2* bands of WISE. We directly selected the UCD samples from this catalogue in the EDF Fornax field.

This catalogue returned 45 late-M dwarfs. We decided to include four extra late-M dwarfs from the *Gaia* UCD catalogue (Reylé 2018). At the end, we have 49 late-M dwarfs (Table B.1). It also returned 29 L dwarfs (Table B.2) and no T dwarf in EDF Fornax. All the L dwarfs are photometrically classified as early-L dwarfs (all of them have a spectral class ≤ L2.0).

Despite no T dwarf being found in EDF Fornax, there is a T6 dwarf WISEA J033921.70–264906.5 (hereafter WISE0339) outside but close to the field (0.34 deg or 20 arcmin away from the northeast border). It is worth including it, considering the large and rectangular FoV of *Euclid*.

We selected an M dwarf, WISE0332, and the T dwarf WISE0339 for spectroscopic characterisation (Table 1). The middle panel in Figure 1 shows the UCD candidates in and near EDF Fornax. The uneven UCD distribution is because the *H*-band VHS only covers about half of EDF Fornax.

## 2.3. Euclid Deep Field South

*Euclid* Deep Field South is a 23 deg<sup>2</sup> octagon stadium-shaped area<sup>3</sup> centered on the coordinate 04h04m57.84s –48°25′22.8″. We directly used the catalogues of Carnero Rosell et al. (2019) and Reylé (2018) as well.

We retrieved 213 late-M dwarfs (Table C.1). Only one late-M dwarf is in the 19 M dwarfs from the *Gaia* UCD catalogue of Reylé (2018). We end up with 231 late-M dwarfs in EDF South.

<sup>3</sup> The envelope of EDF South is 63.25° –45.67°, 65.35° –46.10°, 66.40° –47.25°, 65.99° –48.72°, 59.25° –51.19°, 56.95° –50.82°, 55.90° –49.40°, 56.80° –47.99°.

We retrieved 115 L dwarfs (Table C.2) and two T dwarfs (Table C.3) in EDF South. Ten out of 115 L dwarfs are photometrically classified as mid-L dwarfs (L4.0–L6.0) and the rest are all early-L dwarfs. The two T dwarfs are late-T dwarfs: one T7.0 and the other T8.0. Figure 1 plots all the UCD candidates in EDF South.

## 2.4. Object for coherence check

It is essential to have a shared UCD target to evaluate the coherence between the two facilities. We thus chose a relatively bright L dwarf, WISEA J034209.37–290431.9 (Gagné et al. 2015), close to the EDF Fornax border. This object will still be covered by the EWSs and its position is shown in the middle panel of Figure 1.

## 3. Observations and data reduction

We proposed a long-slit spectroscopic observation on a total of five UCD candidates in EDFs North and Fornax with their spectroscopic standards using the Espectrógrafo Multiobjeto Infra-Rojo (EMIR) on the GTC, programme GTC97-22B (PI J.-Y. Zhang). The Espectrógrafo Multiobjeto Infra-Rojo is a NIR wide-field imager and a multi-object spectrograph with a HAWAII-2 detector. The pixel size is 0.195"/pix. We used a 0.6 arcsec slit with *YJ* and *HK* gratings, covering 0.85 – 1.35 μm and 1.45 – 2.42 μm, respectively, yielding a low spectral resolution of  $R \approx 987$ . We used a standard ABBA observing block sequence. Meanwhile, we asked for a dedicated imaging block of WISE1754 AB in the *J* band with a 7-point dithering pattern before its spectroscopic observation to confirm the companionship. During the spectroscopic observations, we put the slit directly on both objects to obtain their spectra simultaneously. We requested a seeing better than 0.9 arcsec, a clear sky, and no restriction on the moon phase for the GTC observations.

We also proposed a long-slit spectroscopic observation on a total of three UCD candidates in EDF South with spectroscopic standards using the X-shooter (Vernet et al. 2011) on the VLT, ESO programme 112.261S (PI J.-Y. Zhang). The X-shooter consists of three spectroscopic arms: UVB, VIS, and NIR. Each of

the arms is an independent cross-dispersed echelle spectrograph. The UVB arm has an E2V CCD44-82 detector covering  $0.30 - 0.56 \mu\text{m}$  with a pixel scale of  $0.161''/\text{pix}$ ; the VIS arm has a MIT/LL CCID 20 detector covering  $0.56 - 1.02 \mu\text{m}$  with a pixel scale of  $0.158''/\text{pix}$ ; and the NIR arm has a Hawaii 2RG detector covering  $1.02 - 2.48 \mu\text{m}$  with a pixel scale of  $0.258''/\text{pix}$ . We asked for a standard ABBA observing block sequence and simultaneous observations in the three arms. For the UVB arm we used a  $1.3$  arcsec slit ( $R \approx 4100$ ). We used a  $1.2$  arcsec slit for both the VIS arm ( $R \approx 6500$ ) and the NIR arm ( $R \approx 4300$ ). We requested a seeing better than  $1.5$  arcsec, a sky condition of thin cirrus or better, and no restriction on the moon phase for the VLT observations. A summary of all the observations is provided in Table 2.

The 2D EMIR spectral frames were preliminarily reduced by the EMIR default pipeline PyEMIR.<sup>4</sup> The pipeline performed flat field correction, geometric distortion rectification, wavelength calibration (first using the empirical wavelength profile, and then using OH airglow lines in the images to refine the calibration), and ABBA stacking. The outputs are rectified and wavelength-calibrated 2D spectra. We also used the same pipeline to reduce the *J*-band image of WISE1754 AB. The pipeline performed flat field correction, sky subtraction, and stacking under the knowledge of the dithering pattern position. We then extracted 1D spectra in IRAF (Tody 1986).

The *YJ* and *HK* spectra of GTC/EMIR were not observed simultaneously. We convolved and normalised the spectra with the *J* and *H* filter profiles of full throughput of the 2MASS and the VHS.<sup>5</sup> We calculated the *J - H* colour according to the corresponding zero points of each filter. The difference between the observed *J - H* colour and the colour from the spectra is the coefficient that we should apply to adjust the *YJ* and *HK* spectra.

The 2D X-shooter data were reduced by the X-shooter pipeline inside the EsoReflex environment (Freudling et al. 2013). The pipeline produces flux-calibrated 1D spectra for each arm of X-shooter. Then the 1D spectra were corrected for the telluric contribution by Molecfit (Smette et al. 2015; Kausch et al. 2015) in EsoReflex. Because of the low SNR in UVB and VIS arm spectra, we only used NIR arm spectra starting from  $1.02 \mu\text{m}$  in the future analysis.

#### 4. Euclidisation and spectral classification

To ‘Euclidise’ the spectra, we used a Gaussian profile with a full width half maximum (FWHM) of  $40 \text{ \AA}$  to convolve with our spectra ( $R \approx 380$  at  $1.5 \mu\text{m}$ ). We only consider the wavelength range of  $0.92\text{--}1.86 \mu\text{m}$  for our spectra. The results mimic the spectra as if they were taken by the *Euclid* NISP with both blue and red grisms.

We collected the spectral templates from the L and T dwarf data archive<sup>6</sup> of Chiu et al. (2006); Golimowski et al. (2004); Knapp et al. (2004) and the NIRSPEC Brown Dwarf Spectroscopic Survey<sup>7</sup> (BDSS; McLean et al. 2003) to spectroscopically classify L and T dwarfs among our targets. We collected late-M dwarf templates and also early-L dwarf ones from the NASA In-

frared Telescope Facility (IRTF) Spectral Library<sup>8</sup> from Cushing et al. (2005); Rayner et al. (2009).

We normalised both the templates and our spectra. We used linearly distributed sampling points with a step of  $0.1 \text{ \AA}$  in four wavelength ranges:  $1.02\text{--}1.12 \mu\text{m}$ ,  $1.15\text{--}1.34 \mu\text{m}$ ,  $1.47\text{--}1.79 \mu\text{m}$ , and  $1.97\text{--}2.30 \mu\text{m}$  to interpolate our spectra. Ultracool dwarf spectra in the EDFs will be covered by both red and blue grisms; hence, we interpolated the Euclidised spectra without the *K* band, which is not covered by *Euclid*. In particular, to Euclidise the *J*-band spectrum of WISE1745, we used the second wavelength range only. We emphasise that only the red grism will be used in the EWSs. We then interpolated the Euclidised spectra in two ranges:  $1.25\text{--}1.34 \mu\text{m}$  and  $1.47\text{--}1.79 \mu\text{m}$ . We applied the least squares method and found the best fit for the original spectrum and also the Euclidised spectrum of each object. The error was determined by the difference between the spectral subclass of the optimal solution and that of the two nearest points in the template grid.

### 5. Results

#### 5.1. WISE1754 AB

With the *J*-band EMIR image and the images from the PS1 (Figure 2), we excluded the possibility that WISE1754 AB is a co-moving binary system. WISE1754 A has a proper motion in a southeasterly direction, while WISE1754 B does not. The spectroscopy also proves that WISE1754 A is an L1 dwarf, while WISE1754 B is not a UCD at all.

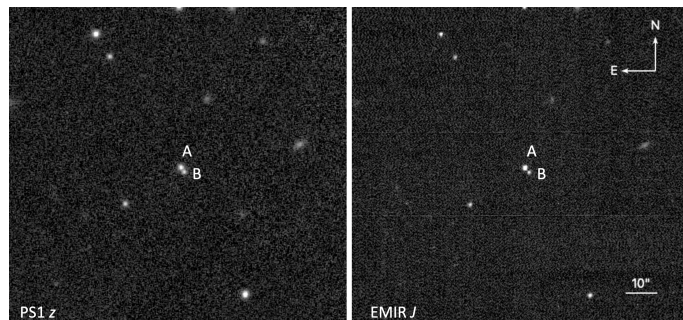


**Fig. 2.** PS1 *z*-band image (left) and GTC/EMIR *J*-band image (right) of WISE1754 AB. The A component has a proper motion towards south-east direction, while the B component does not.

#### 5.2. Common target WISE0342

The GTC/EMIR spectrum and the VLT/X-shooter spectrum exhibit strong agreement with each other, as is indicated in the upper panel of Figure 3. The Euclidised spectra also demonstrate a high degree of similarity, as is illustrated in the middle panel of Figure 3. The differences between two Euclidised spectra are within 0.1 unit of normalised flux, with some spikes of noise around 0.2 (the lower panels of Figure 3). The coherence between the two instruments is good enough to characterise UCDs for *Euclid* in different EDFs.

In comparison with the field dwarf templates, both GTC/EMIR and VLT/X-shooter spectra have two similar local least squares minima at L4.5 and L7.0. The Euclidised

<sup>8</sup> [http://irtfweb.ifa.hawaii.edu/~spex/IRTF\\_Spectral\\_Library/](http://irtfweb.ifa.hawaii.edu/~spex/IRTF_Spectral_Library/)

<sup>4</sup> <https://pyemir.readthedocs.io/en/stable/#>

<sup>5</sup> For the 2MASS: <http://svo2.cab.inta-csic.es/theory/fps3/index.php?mode=browse&gname=2MASS&asttype=>; For the VHS: <http://svo2.cab.inta-csic.es/theory/fps3/index.php?mode=browse&gname=Paranal&gname2=VISTA&asttype=>

<sup>6</sup> <http://svocats.cab.inta-csic.es/chiu06/index.php>

<sup>7</sup> <https://www.astro.ucla.edu/~mclean/BDSSarchive/>.



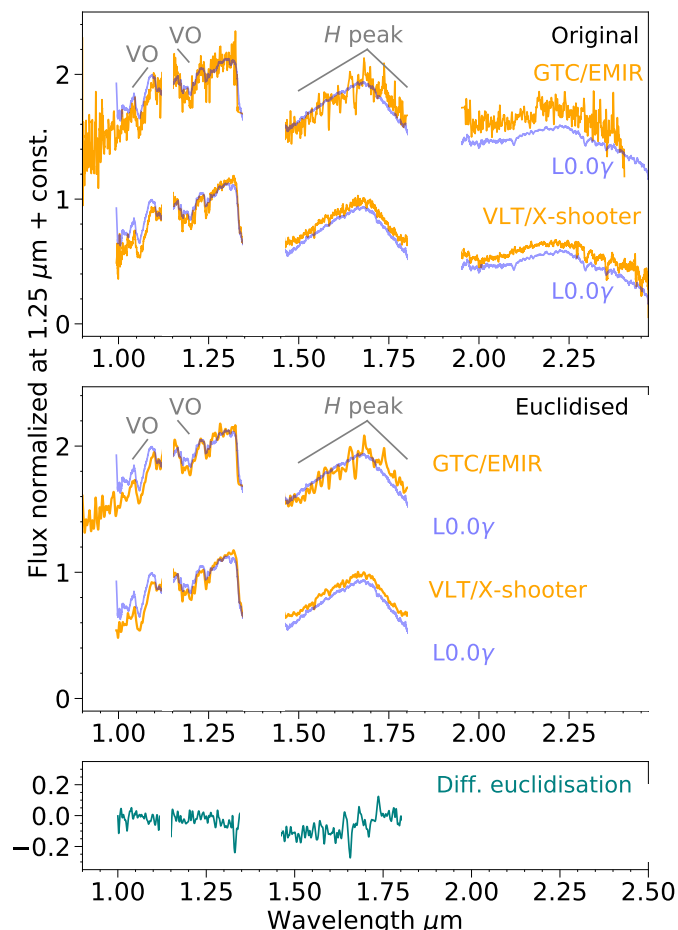


**Fig. 3.** Normalised and Euclidised spectra of W0342 from both GTC/EMIR and the VLT/X-shooter. Strong telluric bands are masked. Features indicating the youth of the object are denoted. Both original spectra were classified as L0.0 $\gamma$  (upper panel). The spectral similarity underscores that GTC/EMIR and the VLT/X-shooter are coherent in characterising UCDs for *Euclid*. The two Euclidised spectra were all classified as L0.0 $\gamma$  (middle panel). The difference between the two Euclidised spectra is visualised in the lower panel.

GTC/EMIR spectrum has been classified as L4.5, and the Euclidised VLT/X-shooter spectrum has two similar local minima of the least squares at L5.5 and L7.0. The confusion of spectral type classification may be due to the youth and, hence, lower surface gravity of the object. For lower-gravity objects, in the *J* band, the FeH feature at 0.99  $\mu\text{m}$ , and the potassium doublets are weaker than those of higher-gravity objects, while the VO absorption features at 1.06 and 1.18  $\mu\text{m}$  are much more prominent. The *H*-band spectrum has a peaked, triangular shape for lower-gravity objects, due to stronger water absorption (Zapatero Osorio et al. 2000; Cushing et al. 2000; Lucas et al. 2001; Gorlova et al. 2003; McGovern et al. 2004; Lodieu et al. 2008; Scholz et al. 2012; Manjavacas et al. 2014; Mužić et al. 2015; Lodieu et al. 2018).

We decided to compare the W0342 spectra against young L $\gamma$ -type UCD templates in the Upper Scorpius association (5–10 Myr) (Lodieu et al. 2018). Our classification suggests a L0.0 $\gamma$  subclass, which agrees with the result of L0 $\beta$  from Gagné et al. (2015), but not with the photometric classification of L4.0 from Carnero Rosell et al. (2019). We demonstrate that *Euclid* slitless spectroscopy will be able to detect spectral indicators sensitive

to the surface gravity or age, at least for late-M to early-L-type UCDs.

### 5.3. Spectral classes

Figure 4 depicts the original spectra and Euclidised spectra of the eight reconnaissance UCDs, except the common target WISE0342 (Figure 3). The best-fit spectral templates are also overplotted. Saturated telluric wavelength regions were masked manually. The results and comparisons of spectral classification are summarised in Table 3. The accuracy of the spectral type depends on the density of the template grid.

The spectral classifications of the reconnaissance UCDs are in line with their photometric spectral classifications from our search and from the selection of Carnero Rosell et al. (2019) and Reylé (2018), except for the young object WISE0342. The Euclidised spectra maintains the spectral classification results. We conclude that *Euclid* NISP slitless spectroscopy using two gratings in the EDFs can bring out an excellent spectral classification for UCDs, with a precision of 0.5 subclass without any major problems. With only the red grism in the EWSs, the spectral classification for mid-L to T dwarfs will be as precise as that in the EDFs; while for those field late-M to early-L dwarfs the precision is of two subclasses because those hotter UCDs have less characteristic features in the *H* band. For young early-L dwarfs like W0342, their peculiar *H* band improves the spectral classification precision of the red grism.

**Table 3.** Summary of the spectral classification.

Name	Phot.	Spec.	Euc.	Euc. red
WISE0332	M9.0	M9.0 $\pm$ 1.0	M9.0 $\pm$ 1.0	M7.0 $\pm$ 1.0
WISE0339	T6.0	T3.5 $\pm$ 0.5	T4.0 $\pm$ 0.5	T3.0 $\pm$ 0.5
WISE0342	L4.0	L0.0 $\pm$ 1.0 $\gamma$	L0.0 $\pm$ 1.0 $\gamma$	L0.0 $\pm$ 1.0 $\gamma$
WISE0352	T7.0	T7.0 $\pm$ 0.5	T7.0 $\pm$ 0.5	T7.0 $\pm$ 0.5
WISE0359	T8.0	T7.5 $\pm$ 0.5	T7.5 $\pm$ 0.5	T7.5 $\pm$ 0.5
WISE0402	L5.0	L4.5 $\pm$ 0.5	L4.5 $\pm$ 0.5	L4.5 $\pm$ 0.5
WISE1745	-	T7.0 $\pm$ 0.5	T7.0 $\pm$ 0.5	-
WISE1754 A	L	L1.0 $\pm$ 0.5	L1.0 $\pm$ 0.5	M9.0 $\pm$ 1.0
WISE1757	M7.0	M9.0 $\pm$ 1.0	M9.0 $\pm$ 1.0	M7.0 $\pm$ 1.0

**Note:** Candidates are ordered by right ascension. Euc. means that the results are derived from the whole Euclidised spectra (for UCDs in the EDFs); and Euc red means only the part covered by the red grism was used (for UCDs in the EWSs).

### 5.4. Sample purity

We selected eight UCD candidates from the whole sample pool for the spectroscopy and all of them were spectroscopically confirmed as UCDs. Assuming an overall purity of our selections in the three EDFs is  $p$ , the probability  $P(X = k, n)$  with  $k$  true UCD in  $n$  candidates follows a binomial distribution,

$$P(X = k, n) = \frac{n!}{k!(n-k)!} p^k (1-p)^{n-k}. \quad (1)$$

Hence, we estimated a 90% confidence interval (with only a lower tail) of the purity by  $P(X = 8, 8) = p^8 \geq 1 - 90\%$ , yielding  $75\% \leq p \leq 100\%$ . The lower limit is extremely conservative since it is completely based on our spectroscopic confirmation.

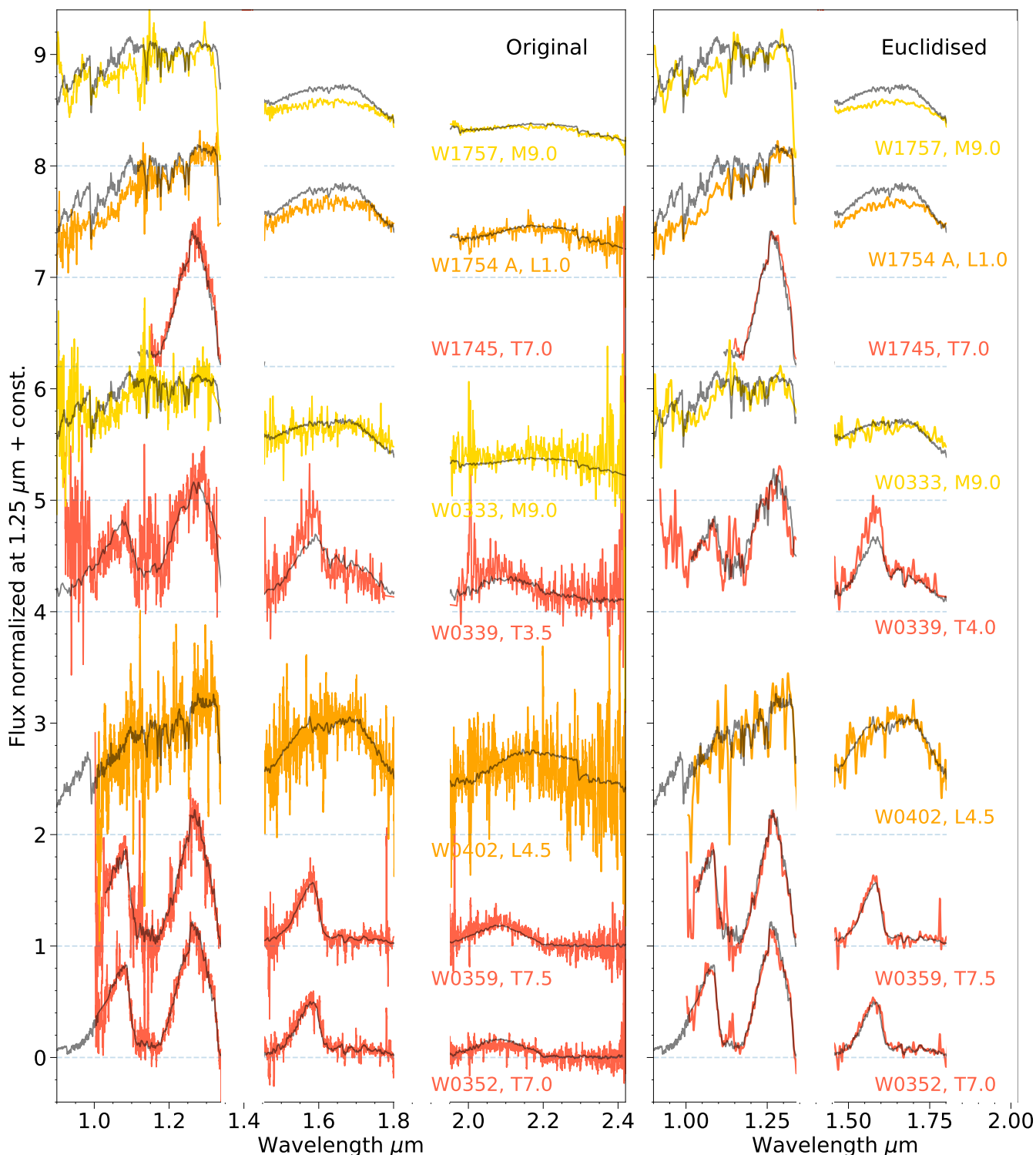


**Fig. 4.** Normalised UCD spectra in the three EDFs. From the top to the bottom are UCDs from EDFs North, Fornax, and South, respectively. The VLT/X-shooter and GTC/EMIR spectra were smoothed with a 31 and 5-pixel-size window, respectively. All the spectra were classified into spectral subclasses, and the best-fit templates are plotted in grey (left panel). We Euclidised the spectra and the classifications remain consistent within 0.5 subclasses (right panel).

## 6. Conclusions

*Euclid*, a space-borne telescope dedicated to cosmology, will also be powerful for UCD science. It has advantages compared with other current space telescopes, especially the combination of its big FoV and its depth in the NIR range. It will start nominal surveys soon and will visit the three EDFs repeatedly. In this

work, we provide a list of UCDs in the three EDFs for *Euclid* to characterise them and use them as references to identify new UCDs. We found 81 (49, 231) M, eight (29, 115) L, and one (0, 2) T dwarfs in EDFs North, Fornax, and South, respectively. The total number of these potential UCD standards is enough to provide a fairly good connection between *Euclid* and ground-based

data, despite the possibility of photometric or spectroscopic variability of any single object.

From the candidate list in or next to all the EDFs, we selected in total eight UCD candidates of different spectral classes, for which we collected spectra with GTC/EMIR and the VLT/X-shooter, confirming their UCD nature. We used a common object, W0342, to demonstrate that these two telescopic instrument combinations provide a coherent UCD characterisation for *Euclid*. All of the eight selected candidates were spectroscopically confirmed as UCDs, suggesting a high UCD purity of the selection that we made. Together with a *J*-band spectrum of a T dwarf in EDF North from the literature, these nine UCD spectra will serve as reconnaissance spectra for UCD discoveries of *Euclid*. We estimated the spectral classification ability of *Euclid* by analysing Euclidised spectra and comparing them to the original spectra. We concluded that *Euclid* NISP spectroscopy will be able to deliver a precise spectral class for UCDs in the EDFs, and to determine their age groups.

At the end of the *Euclid* mission, with about 40–50 visits in each EDF, the co-added spectra will have an SNR at least six times better than the spectra from a single epoch. This may even permit a radial velocity measurement for many UCDs. Their parallaxes and proper motions will be also measured through multi-epoch astrometry. Multi-epoch and multi-band photometry will enable one to monitor the monthly photometric variability of UCDs, which could be caused by magnetic activity, inhomogeneous cloud distribution, rotation, or complex atmosphere dynamics. Combining the determination of spectral classes, distances, kinematics, long-term photometric variabilities, and the ages of thousands of new UCD discoveries, the *Euclid* deep surveys will bring us to a new era in UCD science, with unprecedented statistics for the understanding of the lowest-mass population in the Milky Way.

*Acknowledgements.* We thank the referee for the useful and insightful report. NL acknowledges support from the Agencia Estatal de Investigación del Ministerio de Ciencia e Innovación (AEI-MCINN) under grant PID2019-109522GB-C53. Funding for this research was provided by the European Union (ERC, SUBSTELLAR, project number 101054354). Based on observations made with the Gran Telescopio Canarias (GTC), installed at the Spanish Observatorio del Roque de los Muchachos of the Instituto de Astrofísica de Canarias, on the island of La Palma. Based on observations collected at the European Southern Observatory under ESO programme 112.261S. This research has made use of the Spanish Virtual Observatory (<https://svo.cab.inta-csic.es>) project funded by MCIN/AEI/10.13039/501100011033/ through grant PID2020-112949GB-I00. This work has used the Pan-STARRS1 Surveys (PS1) and the PS1 public science archive that have been made possible through contributions by the Institute for Astronomy, the University of Hawaii, the Pan-STARRS Project Office, the Max-Planck Society and its participating institutes, the Max Planck Institute for Astronomy, Heidelberg and the Max Planck Institute for Extraterrestrial Physics, Garching, The Johns Hopkins University, Durham University, the University of Edinburgh, the Queen's University Belfast, the Harvard-Smithsonian Center for Astrophysics, the Las Cumbres Observatory Global Telescope Network Incorporated, the National Central University of Taiwan, the Space Telescope Science Institute, the National Aeronautics and Space Administration under Grant No. NNX08AR22G issued through the Planetary Science Division of the NASA Science Mission Directorate, the National Science Foundation Grant No. AST-1238877, the University of Maryland, Eotvos Lorand University (ELTE), the Los Alamos National Laboratory, and the Gordon and Betty Moore Foundation. This publication makes use of data products from the Wide-field Infrared Survey Explorer, which is a joint project of the University of California, Los Angeles, and the Jet Propulsion Laboratory/California Institute of Technology, funded by the National Aeronautics and Space Administration. This project used public archival data from the Dark Energy Survey (DES). Funding for the DES Projects has been provided by the U.S. Department of Energy, the U.S. National Science Foundation, the Ministry of Science and Education of Spain, the Science and Technology Facilities Council of the United Kingdom, the Higher Education Funding Council for England, the National Center for Supercomputing Applications at the University of Illinois at Urbana-Champaign, the Kavli Institute of Cosmological Physics at the University of Chicago, the Center for Cosmology and Astro-Particle Physics at the Ohio State University, the Mitchell Institute for

Fundamental Physics and Astronomy at Texas A&M University, Financiadora de Estudos e Projetos, Fundação Carlos Chagas Filho de Amparo à Pesquisa do Estado do Rio de Janeiro, Conselho Nacional de Desenvolvimento Científico e Tecnológico and the Ministério da Ciência, Tecnologia e Inovação, the Deutsche Forschungsgemeinschaft and the Collaborating Institutions in the Dark Energy Survey. The Collaborating Institutions are Argonne National Laboratory, the University of California at Santa Cruz, the University of Cambridge, Centro de Investigaciones Energéticas, Medioambientales y Tecnológicas–Madrid, the University of Chicago, University College London, the DES-Brazil Consortium, the University of Edinburgh, the Eidgenössische Technische Hochschule (ETH) Zürich, Fermi National Accelerator Laboratory, the University of Illinois at Urbana-Champaign, the Institut de Ciències de l'Espai (IEEC/CSIC), the Institut de Física d'Altes Energies, Lawrence Berkeley National Laboratory, the Ludwig-Maximilians Universität München and the associated Excellence Cluster Universe, the University of Michigan, the National Optical Astronomy Observatory, the University of Nottingham, The Ohio State University, the OzDES Membership Consortium, the University of Pennsylvania, the University of Portsmouth, SLAC National Accelerator Laboratory, Stanford University, the University of Sussex, and Texas A&M University. This work made use of Astropy:<sup>9</sup> a community-developed core Python package and an ecosystem of tools and resources for astronomy (Astropy Collaboration et al. 2013, 2018, 2022).

## References

- Aganze, C., Burgasser, A. J., Malkan, M., et al. 2022a, *ApJ*, 924, 114  
 Aganze, C., Burgasser, A. J., Malkan, M., et al. 2022b, *ApJ*, 934, 73  
 Astropy Collaboration, Price-Whelan, A. M., Lim, P. L., et al. 2022, *ApJ*, 935, 167  
 Astropy Collaboration, Price-Whelan, A. M., Sipőcz, B. M., et al. 2018, *AJ*, 156, 123  
 Astropy Collaboration, Robitaille, T. P., Tollerud, E. J., et al. 2013, *A&A*, 558, A33  
 Beiler, S. A., Cushing, M. C., Kirkpatrick, J. D., et al. 2023, *ApJ*, 951, L48  
 Burgasser, A. J., Bezanson, R., Labbe, I., et al. 2024, *ApJ*, 962, 177  
 Burgasser, A. J., Geballe, T. R., Leggett, S. K., Kirkpatrick, J. D., & Golimowski, D. A. 2006, *ApJ*, 637, 1067  
 Burgasser, A. J., Kirkpatrick, J. D., Brown, M. E., et al. 2002, *ApJ*, 564, 421  
 Burgasser, A. J., Logsdon, S. E., Gagné, J., et al. 2015, *ApJS*, 220, 18  
 Carnero Rosell, A., Santiago, B., dal Ponte, M., et al. 2019, *MNRAS*, 489, 5301  
 Chambers, K. C., Magnier, E. A., Metcalfe, N., et al. 2016, arXiv e-prints, arXiv:1612.05560  
 Chiu, K., Fan, X., Leggett, S. K., et al. 2006, *AJ*, 131, 2722  
 Cooper, W. J., Smart, R. L., Jones, H. R. A., & Sarro, L. M. 2024, *MNRAS*, 527, 1521  
 Cushing, M. C. 2014, in *Astrophysics and Space Science Library*, Vol. 401, 50  
 Years of Brown Dwarfs, ed. V. Joergens, 113  
 Cushing, M. C., Kirkpatrick, J. D., Gelino, C. R., et al. 2011, *ApJ*, 743, 50  
 Cushing, M. C., Kirkpatrick, J. D., Gelino, C. R., et al. 2014, *AJ*, 147, 113  
 Cushing, M. C., Rayner, J. T., & Vacca, W. D. 2005, *ApJ*, 623, 1115  
 Cushing, M. C., Tokunaga, A. T., & Kobayashi, N. 2000, *AJ*, 119, 3019  
 Cutri, R. M., Skrutskie, M. F., van Dyk, S., et al. 2003, 2MASS All Sky Catalog of point sources.  
 Cutri, R. M., Wright, E. L., Conrow, T., et al. 2021, *VizieR Online Data Catalog*, II/328  
 Dark Energy Survey Collaboration, Abbott, T., Abdalla, F. B., et al. 2016, *MNRAS*, 460, 1270  
 Delorme, P., Delfosse, X., Albert, L., et al. 2008, *A&A*, 482, 961  
 Euclid Collaboration, Barnett, R., Warren, S. J., et al. 2019, *A&A*, 631, A85  
 Euclid Collaboration, Gabarra, L., Mancini, C., et al. 2023, *A&A*, 676, A34  
 Euclid Collaboration, Moneti, A., McCracken, H. J., et al. 2022a, *A&A*, 658, A126  
 Euclid Collaboration, Scaramella, R., Amiaux, J., et al. 2022b, *A&A*, 662, A112  
 Euclid Collaboration, Schirmer, M., Jahnke, K., et al. 2022c, *A&A*, 662, A92  
 Freudling, W., Romaniello, M., Bramich, D. M., et al. 2013, *A&A*, 559, A96  
 Gagné, J., Faherty, J. K., Cruz, K. L., et al. 2015, *ApJS*, 219, 33  
 Gaia Collaboration, Prusti, T., de Bruijne, J. H. J., et al. 2016, *A&A*, 595, A1  
 Geballe, T. R., Knapp, G. R., Leggett, S. K., et al. 2002, *ApJ*, 564, 466  
 Golimowski, D. A., Leggett, S. K., Marley, M. S., et al. 2004, *AJ*, 127, 3516  
 Gorlova, N. I., Meyer, M. R., Rieke, G. H., & Liebert, J. 2003, *ApJ*, 593, 1074  
 Hainline, K. N., Helton, J. M., Johnson, B. D., et al. 2023, arXiv e-prints, arXiv:2309.03250  
 Holwerda, B., Pirzkal, N., Burgasser, A., & Hsu, C.-C. 2023, arXiv e-prints, arXiv:2306.12363  
 Holwerda, B. W., Hsu, C.-C., Hathi, N., et al. 2024, *MNRAS*, 529, 1067  
 Holwerda, B. W., Trenti, M., Clarkson, W., et al. 2014, *ApJ*, 788, 77

<sup>9</sup> <http://www.astropy.org>



- Hsu, C.-C., Burgasser, A. J., Theissen, C. A., et al. 2021, *ApJS*, 257, 45
- Kausch, W., Noll, S., Smette, A., et al. 2015, *A&A*, 576, A78
- Kirkpatrick, J. D., Cushing, M. C., Gelino, C. R., et al. 2011, *ApJS*, 197, 19
- Kirkpatrick, J. D., Gelino, C. R., Faherty, J. K., et al. 2021, *ApJS*, 253, 7
- Kirkpatrick, J. D., Henry, T. J., & Irwin, M. J. 1997, *AJ*, 113, 1421
- Kirkpatrick, J. D., Henry, T. J., & Simons, D. A. 1995, *AJ*, 109, 797
- Kirkpatrick, J. D., Reid, I. N., Liebert, J., et al. 1999, *ApJ*, 519, 802
- Kirkpatrick, J. D., Reid, I. N., Liebert, J., et al. 2000, *AJ*, 120, 447
- Knapp, G. R., Leggett, S. K., Fan, X., et al. 2004, *AJ*, 127, 3553
- Langeroodi, D. & Hjorth, J. 2023, *ApJ*, 957, L27
- Laureijs, R., Amiaux, J., Arduini, S., et al. 2011, arXiv e-prints, arXiv:1110.3193
- Leggett, S. K., Golimowski, D. A., Fan, X., Geballe, T. R., & Knapp, G. R. 2003, in *Cambridge Workshop on Cool Stars, Stellar Systems, and the Sun*, Vol. 12, *The Future of Cool-Star Astrophysics: 12th Cambridge Workshop on Cool Stars, Stellar Systems, and the Sun*, ed. A. Brown, G. M. Harper, & T. R. Ayres, 120–127
- Li, J., Smith, M. C., Zhong, J., et al. 2016, *ApJ*, 823, 59
- Lodieu, N., Hambly, N. C., Jameson, R. F., & Hodgkin, S. T. 2008, *MNRAS*, 383, 1385
- Lodieu, N., Zapatero Osorio, M. R., Béjar, V. J. S., & Peña Ramírez, K. 2018, *MNRAS*, 473, 2020
- Lucas, P. W., Roche, P. F., Allard, F., & Hauschildt, P. H. 2001, *MNRAS*, 326, 695
- Luhman, K. L. 2014, *ApJ*, 786, L18
- Mace, G. N., Kirkpatrick, J. D., Cushing, M. C., et al. 2013, *ApJS*, 205, 6
- Manjavacas, E., Bonnefoy, M., Schlieder, J. E., et al. 2014, *A&A*, 564, A55
- Manjavacas, E., Tremblin, P., Birkmann, S., et al. 2024, arXiv e-prints, arXiv:2402.04230
- Martín, E. L., Basri, G., Delfosse, X., & Forveille, T. 1997, *A&A*, 327, L29
- Martín, E. L., Basri, G., Zapatero-Osorio, M. R., Rebolo, R., & López, R. J. G. 1998, *ApJ*, 507, L41
- Martín, E. L., Delfosse, X., Basri, G., et al. 1999, *AJ*, 118, 2466
- Martín, E. L., Zhang, J. Y., Esparza, P., et al. 2021, *A&A*, 655, L3
- McGovern, M. R., Kirkpatrick, J. D., McLean, I. S., et al. 2004, *ApJ*, 600, 1020
- McLean, I. S., Becklin, E. E., Bendiksen, O., et al. 1998, in *Society of Photo-Optical Instrumentation Engineers (SPIE) Conference Series*, Vol. 3354, *Infrared Astronomical Instrumentation*, ed. A. M. Fowler, 566–578
- McLean, I. S., Graham, J. R., Becklin, E. E., et al. 2000, in *Society of Photo-Optical Instrumentation Engineers (SPIE) Conference Series*, Vol. 4008, *Optical and IR Telescope Instrumentation and Detectors*, ed. M. Iye & A. F. Moorwood, 1048–1055
- McLean, I. S., McGovern, M. R., Burgasser, A. J., et al. 2003, *ApJ*, 596, 561
- McMahon, R. G., Banerji, M., Gonzalez, E., et al. 2013, *The Messenger*, 154, 35
- Mužić, K., Scholz, A., Geers, V. C., & Jayawardhana, R. 2015, *ApJ*, 810, 159
- Nonino, M., Glazebrook, K., Burgasser, A. J., et al. 2023, *ApJ*, 942, L29
- Pirzkal, N., Burgasser, A. J., Malhotra, S., et al. 2009, *ApJ*, 695, 1591
- Pirzkal, N., Sahu, K. C., Burgasser, A., et al. 2005, *ApJ*, 622, 319
- Rayner, J. T., Cushing, M. C., & Vacca, W. D. 2009, *ApJS*, 185, 289
- Reylé, C. 2018, *A&A*, 619, L8
- Rhodes, J., Nichol, R. C., Aubourg, É., et al. 2017, *ApJS*, 233, 21
- Ryan, R. E., J., Hathi, N. P., Cohen, S. H., & Windhorst, R. A. 2005, *ApJ*, 631, L159
- Ryan, R. E., Thorman, P. A., Yan, H., et al. 2011, *ApJ*, 739, 83
- Sarro, L. M., Berihuete, A., Smart, R. L., et al. 2023, *A&A*, 669, A139
- Schmidt, S. J., Hawley, S. L., West, A. A., et al. 2015, *AJ*, 149, 158
- Scholz, A., Muzic, K., Geers, V., et al. 2012, *ApJ*, 744, 6
- Skrutskie, M. F., Cutri, R. M., Stiening, R., et al. 2006, *AJ*, 131, 1163
- Skrzypek, N., Warren, S. J., & Faherty, J. K. 2016, *A&A*, 589, A49
- Smette, A., Sana, H., Noll, S., et al. 2015, *A&A*, 576, A77
- Solano, E., Gálvez-Ortiz, M. C., Martín, E. L., et al. 2021, *MNRAS*, 501, 281
- Stanway, E. R., Bremer, M. N., Lehnert, M. D., & Eldridge, J. J. 2008, *MNRAS*, 384, 348
- Stevenson, A. T., Haswell, C. A., Barnes, J. R., & Barstow, J. K. 2023, *MNRAS*, 526, 5155
- Taylor, M. B. 2005, in *Astronomical Society of the Pacific Conference Series*, Vol. 347, *Astronomical Data Analysis Software and Systems XIV*, ed. P. Shopbell, M. Britton, & R. Ebert, 29
- Tody, D. 1986, in *Society of Photo-Optical Instrumentation Engineers (SPIE) Conference Series*, Vol. 627, *Instrumentation in astronomy VI*, ed. D. L. Crawford, 733
- van Vledder, I., van der Vlugt, D., Holwerda, B. W., et al. 2016, *MNRAS*, 458, 425
- Vernet, J., Dekker, H., D’Odorico, S., et al. 2011, *A&A*, 536, A105
- Wang, P.-Y., Goto, T., Ho, S. C. C., et al. 2023, *MNRAS*, 523, 4534
- Wright, E. L., Eisenhardt, P. R. M., Mainzer, A. K., et al. 2010, *AJ*, 140, 1868
- Zapatero Osorio, M. R., Béjar, V. J. S., Martín, E. L., et al. 2000, *Science*, 290, 103

**Appendix A: Lists of ultracool dwarf candidates in Euclid Deep Field North**
**Table A.1.** 81 late-M-type UCD candidates as photometric standards in EDF North and their photometry measurements.

$\alpha$ (hms.ss)	$\delta$ (dms.s)	$i$	$z$	$Y$	$J$	$H$	$K$	W1	W2
17:35:39.86	+65:35:41.7	18.79±0.01	17.84±0.01	17.35±0.01	15.99±0.08	15.3±0.09	15.09±0.16	14.69±0.01	14.52±0.02
17:36:03.27	+65:35:11.8	18.53±0.0	17.61±0.01	17.14±0.01	15.81±0.07	15.24±0.09	14.71±0.12	14.64±0.01	14.4±0.04
17:36:24.77	+65:57:35.1	18.64±0.01	17.55±0.01	17.02±0.01	15.68±0.08	15.05±0.1	14.51±0.11	14.31±0.01	13.9±0.01
17:37:25.84	+66:00:00.3	19.47±0.01	18.51±0.01	18.02±0.02	16.47±0.14	15.73±0.18	15.36	15.23±0.04	14.94±0.04
17:38:31.21	+65:57:25.7	18.19±0.01	17.07±0.0	16.42±0.0	14.83±0.04	14.25±0.05	13.92±0.07	13.61±0.01	13.39±0.01
17:38:36.60	+66:53:18.8	19.15±0.01	18.26±0.01	17.77±0.02	16.38±0.13	15.84±0.19	15.4±0.21	14.95±0.03	14.68±0.06
17:41:18.44	+65:51:41.9	19.01±0.01	17.9±0.01	17.32±0.01	15.93±0.08	15.45±0.09	15.19±0.17	14.74±0.03	14.51±0.03
17:42:40.51	+66:14:24.9	17.86±0.0	16.79±0.0	16.23±0.01	14.76±0.04	14.11±0.05	13.79±0.05	13.47±0.01	13.3±0.01
17:43:02.14	+66:42:00.9	17.66±0.0	16.46±0.0	15.79±0.01	14.25±0.03	13.6±0.04	13.2±0.04	12.95±0.01	12.76±0.01
17:45:02.13	+67:10:45.6	19.74±0.01	18.36±0.0	17.56±0.01	16.01±0.09	15.24±0.11	14.77±0.12	14.12±0.02	13.84±0.03
17:46:07.58	+67:43:13.1	19.24±0.01	18.3±0.01	17.79±0.01	16.51±0.12	15.94±0.19	15.35±0.22	15.27±0.04	15.13±0.07
17:46:33.48	+67:31:15.2	19.28±0.01	18.51±0.01	18.14±0.03	16.58±0.12	16.05±0.21	15.41±0.2	15.24±0.03	15.07±0.06
17:47:13.27	+65:48:49.8	19.28±0.02	18.52±0.04	18.22±0.05	16.29±0.11	15.71±0.13	14.89	14.93±0.02	14.72±0.05
17:47:28.29	+64:42:49.5	18.77±0.01	17.91±0.04	17.47±0.02	16.09±0.09	15.3±0.09	14.9±0.13	14.83±0.03	14.59±0.03
17:48:14.55	+64:31:37.9	19.83±0.01	18.82±0.02	18.37±0.03	17.01±0.21	16.15±0.17	15.77±0.28	15.93±0.07	15.61±0.08
17:48:55.26	+67:08:18.0	19.98±0.01	18.87±0.01	18.19±0.01	16.54±0.14	15.98±0.18	15.49±0.22	14.79±0.02	14.52±0.03
17:51:02.52	+66:26:00.3	18.88±0.01	18.01±0.01	17.55±0.01	16.13±0.09	15.56±0.14	15.28±0.18	14.65±0.02	14.43±0.03
17:51:14.75	+64:57:18.9	18.62±0.01	17.71±0.01	17.26±0.01	15.9±0.08	15.41±0.1	14.89±0.13	14.63±0.02	14.49±0.04
17:51:19.39	+64:05:47.2	19.33±0.01	18.15±0.02	17.54±0.01	16.05±0.09	15.31±0.09	14.89±0.14	14.61±0.01	14.37±0.03
17:51:38.41	+65:40:14.9	19.54±0.02	18.7±0.01	18.23±0.02	16.72±0.15	16.22±0.21	15.56±0.24	15.55±0.05	15.21±0.07
17:51:42.95	+68:20:11.9	19.34±0.02	18.32±0.02	17.81±0.01	16.54±0.12	15.65±0.13	15.19±0.18	15.27±0.03	15.14±0.05
17:51:50.30	+64:54:32.0	18.54±0.01	17.58±0.0	17.07±0.01	15.7±0.06	15.08±0.08	14.66±0.12	13.96±0.01	13.81±0.04
17:53:23.33	+66:53:29.8	19.42±0.01	18.47±0.01	17.97±0.02	16.68±0.15	15.91±0.17	15.47±0.17	14.78±0.03	14.54±0.03
17:53:58.60	+65:26:58.2	17.58±0.0	16.66±0.0	16.2±0.01	14.84±0.04	14.18±0.05	13.83±0.06	13.55±0.01	13.38±0.01
<sup>(1)</sup> 17:54:40.48	+64:08:09.2	16.31±0.0	15.2±0.0	14.64±0.01	13.12±0.02	12.59±0.02	12.27±0.03	12.01±0.02	11.78±0.02
17:55:15.62	+66:54:22.8	18.67±0.01	17.41±0.01	16.75±0.01	15.24±0.05	14.57±0.05	14.22±0.09	13.94±0.01	13.8±0.02
17:55:15.85	+64:10:51.3	17.44±0.0	16.5±0.01	16.02±0.0	14.58±0.03	14.01±0.04	13.65±0.05	13.11±0.01	12.97±0.01
17:56:08.33	+67:10:36.7	19.31±0.01	18.2±0.01	17.66±0.01	16.25±0.11	15.58±0.12	15.2±0.19	15.09±0.02	14.86±0.04
17:56:26.28	+63:52:07.1	16.92±0.0	16.04±0.0	15.59±0.0	14.23±0.03	13.61±0.03	13.4±0.04	12.87±0.01	12.7±0.01
17:56:49.34	+68:25:57.2	18.59±0.01	17.71±0.01	17.22±0.01	15.85±0.08	15.35±0.11	14.8±0.13	14.7±0.02	14.45±0.04
<b>17:57:30.73</b>	<b>+67:41:40.1</b>	<b>16.86±0.0</b>	<b>15.74±0.01</b>	<b>15.15±0.01</b>	<b>13.7±0.03</b>	<b>13.15±0.02</b>	<b>12.74±0.03</b>	<b>12.53±0.01</b>	<b>12.32±0.01</b>
17:57:31.04	+64:39:19.1	19.16±0.0	18.48±0.01	18.2±0.01	16.47±0.12	15.89±0.16	14.66	14.95±0.03	14.79±0.03
17:57:35.66	+67:18:52.0	19.77±0.02	18.59±0.02	17.92±0.02	16.51±0.14	15.82±0.15	15.22±0.2	15.1±0.03	14.9±0.05
17:57:55.04	+64:18:05.7	19.95±0.01	18.59±0.01	17.78±0.02	16.23±0.09	15.13±0.07	14.61±0.1	14.46±0.01	14.32±0.05
17:58:35.99	+65:43:06.2	18.44±0.0	17.46±0.01	16.95±0.0	15.63±0.06	14.92±0.07	14.7±0.11	14.34±0.01	14.12±0.02
17:59:13.72	+65:24:09.2	20.28±0.02	19.04±0.01	18.28±0.01	16.82±0.15	15.95±0.17	15.47±0.21	15.07±0.05	14.9±0.08
18:00:56.18	+65:52:23.1	19.1±0.01	17.74±0.01	16.93±0.01	15.22±0.04	14.53±0.04	14.17±0.06	13.8±0.01	13.59±0.01
18:01:09.10	+63:53:39.4	19.42±0.01	18.49±0.01	17.87±0.06	16.53±0.11	15.95±0.14	15.23±0.16	15.44±0.05	15.16±0.08
18:01:41.24	+64:00:09.7	19.48±0.01	18.57±0.01	18.11±0.02	16.6±0.11	16.03±0.16	15.57±0.22	15.19±0.04	14.89±0.05
18:01:55.15	+67:37:03.2	19.24±0.01	18.32±0.01	17.84±0.01	16.49±0.13	15.72±0.14	15.5	15.07±0.03	14.87±0.04
18:02:13.83	+65:00:21.3	18.88±0.0	18.03±0.01	17.56±0.01	16.14±0.07	15.62±0.11	15.04±0.12	14.9±0.03	14.69±0.05
18:02:30.40	+67:00:13.8	19.04±0.01	18.16±0.01	17.68±0.01	16.28±0.12	15.78±0.17	15.38±0.23	14.88±0.01	14.67±0.05
18:02:40.56	+65:46:26.9	19.97±0.01	18.96±0.01	18.4±0.02	17.07±0.18	16.08±0.15	15.72±0.23	15.29±0.03	15.01±0.04
<sup>(1)</sup> 18:03:14.25	+65:32:08.1	18.77±0.01	17.65±0.0	17.05±0.01	15.54±0.05	14.85±0.06	14.47±0.08	14.37±0.03	14.17±0.03
18:03:29.52	+65:02:28.2	19.85±0.01	18.83±0.02	18.26±0.01	16.8±0.13	16.23±0.18	15.84	15.34±0.02	15.19±0.09
18:03:51.03	+66:48:06.4	19.26±0.01	18.28±0.01	17.76±0.01	16.35±0.11	15.73±0.13	14.84	15.16±0.02	14.93±0.04
18:04:38.48	+64:40:30.2	20.44±0.03	19.28±0.02	18.63±0.03	17.23±0.19	16.11±0.16	15.76±0.25	15.82±0.05	15.66±0.08
18:04:40.83	+65:03:30.8	19.14±0.01	18.32±0.01	17.88±0.01	16.41±0.11	15.94±0.13	15.4	15.56±0.03	15.03±0.04
18:04:41.87	+65:27:06.9	20.22±0.02	19.35±0.03	18.92±0.04	17.33±0.22	16.55±0.23	15.58±0.21	16.01±0.05	15.71±0.1
18:05:03.33	+63:53:26.6	19.8±0.01	18.78±0.01	18.25±0.01	16.79±0.14	16.1±0.17	15.68	15.53±0.02	15.27±0.07
18:05:32.10	+68:20:01.8	19.63±0.01	18.55±0.01	17.95±0.02	16.27±0.11	15.67±0.12	15.2	15.0±0.03	14.72±0.05
18:05:41.60	+63:38:17.8	20.24±0.02	19.09±0.02	18.47±0.02	16.77±0.14	16.22±0.19	15.36±0.18	15.21±0.03	15.02±0.05
18:05:44.81	+66:22:59.8	19.92±0.01	18.77±0.02	18.12±0.02	16.78±0.15	15.82±0.14	15.03	14.97±0.01	14.73±0.04
18:06:01.72	+67:53:11.4	19.47±0.01	18.6±0.01	18.11±0.02	16.67±0.15	16.04±0.18	15.34	15.53±0.03	15.27±0.07
18:06:15.25	+65:23:25.6	19.39±0.01	18.44±0.01	17.88±0.01	16.44±0.11	15.96±0.15	15.4	15.03±0.02	14.82±0.05
18:06:59.30	+66:10:51.6	18.81±0.01	17.88±0.01	17.47±0.01	16.13±0.09	15.48±0.11	15.27±0.19	14.47±0.04	14.28±0.04
18:07:34.58	+64:02:22.5	19.73±0.01	18.76±0.02	18.28±0.02	16.96±0.15	15.9	15.57±0.19	15.36±0.03	15.12±0.06
18:08:08.20	+67:01:09.7	19.09±0.0	18.18±0.01	17.73±0.01	16.27±0.1	15.65±0.12	15.36±0.22	14.48±0.02	14.2±0.03
18:08:45.44	+64:06:22.1	19.82±0.01	18.59±0.02	17.93±0.02	16.43±0.11	15.85±0.13	15.4±0.19	14.99±0.02	14.84±0.04
18:08:51.52	+68:00:04.3	17.95±0.0	17.02±0.01	16.46±0.01	15.09±0.04	14.51±0.05	14.1±0.07	13.73±0.01	13.52±0.01
18:09:34.21	+66:21:13.5	19.18±0.01	18.15±0.01	17.6±0.01	16.16±0.09	15.55±0.11	15.29±0.21	14.96±0.02	14.77±0.05
18:09:34.94	+66:21:41.2	19.03±0.02	17.66±0.01	16.89±0.01	15.4±0.05	14.86±0.06	14.39±0.09	14.05±0.01	13.79±0.01
18:09:40.07	+64:48:33.6	19.32±0.01	18.31±0.02	17.78±0.01	16.42±0.11	15.63±0.13	15.23	15.18±0.04	14.91±0.06
18:09:41.00	+63:51:41.2	18.17±0.01	17.15±0.01	16.6±0.01	15.16±0.04	14.59±0.05	14.26±0.07	13.91±0.01	13.76±0.04

**Table A.1.** continued.

$\alpha$ (hhmmss.ss)	$\delta$ (ddmmss.s)	$i$	$z$	$Y$	$J$	$H$	$K$	$W1$	$W2$
18:10:22.13	+64:16:37.5	19.36±0.01	18.48±0.01	18.13±0.02	16.65±0.12	16.02±0.17	15.32	15.26±0.02	15.05±0.07
18:10:22.24	+64:04:37.2	19.06±0.01	18.3±0.02	17.85±0.01	16.35±0.11	15.88±0.15	14.94	15.03±0.03	14.83±0.05
18:10:30.13	+65:13:38.8	19.64±0.01	18.58±0.01	18.07±0.01	16.87±0.15	16.16±0.2	15.55	15.15±0.03	14.91±0.06
18:10:48.82	+65:32:39.9	19.61±0.01	18.79±0.02	18.36±0.03	16.68±0.14	16.1	15.69	14.95±0.02	14.75±0.07
18:12:31.83	+66:41:50.8	16.9±0.0	15.97±0.0	15.51±0.0	14.19±0.03	13.57±0.03	13.3±0.04	13.04±0.01	12.82±0.01
18:13:43.62	+65:48:10.5	19.37±0.01	18.49±0.01	17.95±0.02	16.45±0.1	15.95±0.14	15.39±0.17	15.28±0.02	15.06±0.06
18:15:03.88	+64:24:10.7	19.85±0.01	18.81±0.02	18.25±0.03	16.88±0.14	16.06±0.16	14.99	15.43±0.03	15.24±0.07
18:15:10.85	+64:34:27.8	18.74±0.01	17.64±0.01	17.05±0.01	15.77±0.06	15.02±0.07	14.73±0.1	14.55±0.02	14.36±0.04
18:15:21.44	+64:47:21.3	19.22±0.01	17.99±0.01	17.29±0.01	15.73±0.07	15.06±0.07	14.49±0.08	14.35±0.01	14.15±0.03
18:15:30.11	+67:45:28.7	17.97±0.01	17.04±0.01	16.56±0.01	15.16±0.04	14.58±0.05	14.33±0.09	13.71±0.01	13.5±0.02
18:15:30.92	+67:08:13.7	19.45±0.01	18.42±0.01	17.88±0.02	16.4±0.11	15.62±0.12	15.23	15.18±0.03	15.03±0.07
18:16:08.19	+67:50:26.8	18.71±0.01	17.83±0.01	17.39±0.01	16.02±0.08	15.48±0.11	15.11±0.18	14.62±0.01	14.48±0.05
18:17:15.82	+66:27:00.1	19.29±0.01	18.26±0.0	17.7±0.02	16.25±0.1	15.4±0.1	15.12±0.17	14.93±0.02	14.76±0.05
18:18:18.38	+65:04:30.0	19.43±0.01	18.56±0.01	18.09±0.01	16.67±0.13	16.15±0.17	15.07	15.43±0.06	15.17±0.12
18:20:49.32	+65:47:44.5	18.98±0.01	17.96±0.0	17.41±0.01	16.08±0.09	15.43±0.1	15.06±0.13	14.51±0.02	14.31±0.02
18:21:42.11	+65:37:24.4	19.71±0.01	18.58±0.01	18.05±0.02	16.62±0.14	16.14±0.22	15.13	15.38±0.04	15.22±0.09
18:21:54.00	+66:49:00.2	19.55±0.01	18.67±0.01	18.15±0.01	16.8±0.15	15.98±0.18	15.72±0.24	15.57±0.06	15.28±0.09

**Note:** Objects are listed in the order of RA value. The coordinates are from the 2MASS. The object with bold coordinates is the one selected for the spectroscopy observation.

**References.** (1). Sample only from Reylé (2018), with *Gaia* coordinates,  $i$ ,  $z$ ,  $Y$  photometry from the PS1 and  $J$ ,  $H$ ,  $K$  photometry from the 2MASS.

**Table A.2.** Eight L-type UCD candidates as photometric standards in the EDF North and their photometry measurements.

$\alpha$ (hms.ss)	$\delta$ (dms.s)	$i$	$z$	$Y$	$J$	$H$	$K$	$W1$	$W2$
17:44:09.36	+64:06:39.4	20.86±0.04	19.44±0.02	18.58±0.0	16.79±0.16	15.78±0.14	15.57±0.24	14.81±0.02	14.56±0.04
<b>17:54:10.29</b>	<b>+67:12:11.7</b>	20.35±0.03	18.91±0.02	18.03±0.03	16.13±0.1	15.48±0.12	15.09±0.18	14.77±0.01	14.61±0.05
17:59:47.45	+63:31:24.5	20.53±0.04	19.06±0.01	18.2±0.02	16.51±0.12	15.91±0.15	15.48±0.19	15.22±0.12	14.85±0.07
18:09:04.41	+64:08:44.4	21.03±0.03	19.59±0.04	18.69±0.02	16.73±0.14	16.14±0.17	15.44±0.19	15.03±0.02	14.77±0.06
18:14:40.32	+64:08:50.9	20.17±0.01	18.79±0.01	17.92±0.01	16.19±0.08	15.68±0.11	14.94±0.11	14.76±0.02	14.48±0.05
18:18:32.17	+64:51:17.8	21.02±0.02	19.56±0.02	18.7±0.03	16.91±0.17	16.02±0.14	15.03	15.62±0.15	15.18±0.11
18:19:10.46	+67:16:21.5	20.79±0.02	19.4±0.03	18.45±0.03	16.76±0.16	16.05±0.22	15.25±0.17	15.17±0.04	14.92±0.06
18:19:49.43	+66:00:54.8	20.24±0.02	18.65±0.01	17.62±0.01	15.44±0.06	14.6±0.06	14.13±0.06	13.46±0.01	13.18±0.02

**Note:** Objects are listed in the order of RA value. The coordinates are from the 2MASS. The object with bold coordinates is the one selected for the spectroscopy observation.

## Appendix B: Lists of ultracool dwarf candidates in Euclid Deep Field Fornax

Table B.1. 49 M-type UCD candidates as photometric standards in EDF Fornax and their photometry measurements.

$\alpha$ (hms.ss)	$\delta$ (dms.s)	SpT.	$i$	$z$	$Y$	$J$	$H$	$K$	W1	W2
<sup>(1)</sup> 03:27:11.85	-28:28:23.5	9.0	19.05±0.0	17.55±0.0	17.09±0.0	15.34±0.05	14.62±0.05	14.19±0.06	13.91±0.03	13.65±0.03
<sup>(1)</sup> 03:27:46.17	-29:06:59.5	8.5	17.95±0.0	16.54±0.0	16.09±0.0	14.53±0.04	13.8±0.04	13.41±0.04	13.14±0.02	12.87±0.03
03:29:34.75	-29:11:52.1	8.0	21.15±0.01	19.94±0.01	19.62±0.04	18.02±0.03	17.41±0.03	16.93±0.05	-	-
03:30:13.20	-26:30:18.8	9.0	21.37±0.02	20.05±0.01	19.68±0.04	17.95±0.03	17.48±0.04	17.04±0.06	16.69±0.06	16.74±0.22
03:30:27.26	-27:01:51.5	8.0	21.86±0.03	20.53±0.01	20.21±0.07	18.57±0.06	18.27±0.09	17.73±0.12	18.07±0.18	17.21
03:30:44.91	-26:24:35.0	9.0	22.98±0.07	21.53±0.03	21.29±0.2	19.51±0.13	19.5±0.27	-	-	-
03:31:13.55	-27:27:12.1	9.0	22.62±0.04	21.3±0.02	20.95±0.12	19.24±0.1	18.75±0.14	18.37±0.22	-	-
03:31:33.08	-29:23:41.9	9.0	22.19±0.03	20.82±0.02	20.4±0.07	18.69±0.05	18.04±0.05	17.56±0.08	-	-
03:31:49.70	-26:55:13.0	8.0	20.09±0.01	18.81±0.0	18.5±0.02	16.84±0.01	16.28±0.02	15.9±0.02	15.59±0.03	15.55±0.08
03:31:50.21	-29:30:22.1	9.0	22.86±0.07	21.44±0.04	21.1±0.16	19.46±0.1	18.86±0.12	18.3±0.16	18.15±0.21	17.48
03:31:52.86	-29:20:38.0	8.0	21.82±0.03	20.61±0.02	20.45±0.09	18.66±0.05	18.09±0.06	17.89±0.11	17.54±0.12	17.51
03:32:12.47	-29:46:39.6	8.0	21.77±0.02	20.45±0.02	20.19±0.06	18.45±0.04	18.02±0.06	17.84±0.11	17.35±0.1	16.87±0.24
03:32:14.37	-29:40:20.9	9.0	22.65±0.07	21.19±0.04	20.83±0.17	19.17±0.08	18.8±0.11	17.93±0.12	-	-
03:32:19.94	-28:52:44.3	8.0	20.31±0.01	19.07±0.0	18.75±0.02	17.06±0.02	16.54±0.02	16.1±0.03	15.96±0.04	15.73±0.09
03:32:24.16	-27:42:11.4	8.0	22.26±0.04	21.01±0.02	20.76±0.11	19.06±0.09	18.68±0.13	18.0±0.16	18.15±0.2	17.56
03:32:26.71	-28:02:47.8	9.0	22.04±0.03	20.59±0.01	20.21±0.06	18.46±0.08	18.04±0.09	17.39±0.09	-	-
03:32:27.28	-27:06:59.8	9.0	21.39±0.01	20.06±0.01	19.72±0.04	18.04±0.03	17.43±0.04	17.01±0.06	16.71±0.06	16.06±0.12
03:32:32.52	-28:17:11.7	9.0	22.57±0.05	21.31±0.03	20.98±0.13	19.26±0.15	18.86±0.19	18.42±0.24	17.72±0.13	17.04
03:32:33.19	-26:42:05.7	9.0	20.84±0.01	19.52±0.0	19.19±0.03	17.46±0.02	16.87±0.02	16.48±0.04	16.09±0.05	15.88±0.11
<b>03:32:34.37</b>	<b>-27:33:33.9</b>	9.0	20.54±0.01	19.25±0.0	18.88±0.02	17.2±0.02	16.66±0.02	16.24±0.03	15.84±0.04	15.58±0.08
03:32:34.40	-29:34:01.0	8.0	21.86±0.03	20.61±0.02	20.41±0.09	18.7±0.05	18.09±0.06	17.62±0.09	-	-
03:32:58.14	-27:58:29.9	9.0	22.42±0.04	21.11±0.02	20.85±0.12	18.97±0.12	18.7±0.16	18.25±0.21	17.77±0.14	17.0±0.26
03:32:59.19	-29:26:03.7	8.0	22.09±0.03	20.86±0.02	20.64±0.11	18.99±0.06	18.52±0.09	17.97±0.12	17.85±0.15	17.53
03:33:02.41	-27:09:27.9	9.0	23.12±0.07	21.77±0.04	21.26±0.16	19.66±0.14	19.0±0.17	18.68±0.28	-	-
03:33:18.66	-26:39:31.8	9.0	21.44±0.02	20.1±0.01	19.88±0.05	18.1±0.04	17.54±0.04	17.07±0.06	-	-
03:33:32.76	-29:12:10.5	9.0	22.34±0.04	20.91±0.02	20.64±0.11	18.86±0.06	18.37±0.08	18.06±0.13	17.83±0.15	17.5
03:33:41.46	-29:36:08.7	9.0	21.15±0.01	19.67±0.01	19.33±0.04	17.57±0.02	16.98±0.02	16.53±0.03	16.34±0.05	16.04±0.11
03:33:41.71	-27:24:31.6	8.0	21.0±0.01	19.78±0.01	19.39±0.04	17.74±0.03	17.17±0.03	16.88±0.05	16.44±0.05	16.61±0.21
03:33:53.27	-27:49:15.1	8.0	21.85±0.03	20.56±0.01	20.28±0.07	18.6±0.08	18.29±0.11	17.7±0.13	17.41±0.11	17.41
03:34:06.32	-28:25:05.0	8.0	21.6±0.02	20.32±0.01	20.0±0.05	18.39±0.07	17.68±0.06	17.31±0.09	17.33±0.1	17.23±0.35
03:34:09.89	-26:47:29.5	9.0	22.89±0.06	21.35±0.02	20.96±0.12	19.1±0.09	18.69±0.13	18.48±0.23	18.14±0.21	17.59
03:34:21.38	-26:59:08.5	9.0	21.88±0.02	20.43±0.01	20.2±0.07	18.34±0.05	17.82±0.06	17.46±0.09	17.05±0.08	17.48
03:34:34.36	-29:43:56.3	8.0	21.21±0.01	19.93±0.01	19.68±0.05	18.03±0.03	17.59±0.04	17.25±0.07	17.14±0.09	16.74±0.21
03:34:41.17	-27:46:08.6	9.0	21.86±0.03	20.51±0.01	20.16±0.07	18.39±0.07	17.86±0.08	17.35±0.1	17.13±0.09	16.73±0.21
03:34:50.80	-26:32:31.3	9.0	21.85±0.03	20.56±0.02	20.2±0.08	18.55±0.06	18.03±0.07	17.57±0.11	17.52±0.14	16.61±0.2
03:34:52.21	-27:06:22.1	8.0	21.28±0.02	20.03±0.01	19.7±0.04	18.06±0.04	17.54±0.05	17.15±0.07	17.02±0.08	16.4±0.17
03:34:52.42	-28:04:28.6	8.0	22.52±0.05	21.25±0.03	21.07±0.14	19.22±0.15	18.82±0.18	18.26±0.22	-	-
03:34:56.52	-29:20:19.1	8.0	21.73±0.02	20.48±0.01	20.24±0.07	18.59±0.05	18.12±0.06	17.67±0.11	17.47±0.12	17.33
03:35:07.60	-28:48:25.9	8.0	21.5±0.02	20.22±0.01	20.0±0.07	18.28±0.05	-	-	17.1±0.09	16.95±0.27
03:35:17.37	-28:43:41.4	9.0	21.82±0.01	20.56±0.01	20.34±0.07	18.62±0.07	-	-	16.97±0.08	16.37±0.16
03:35:21.13	-27:43:39.4	9.0	22.31±0.04	20.93±0.02	20.62±0.09	18.89±0.11	-	-	17.62±0.13	17.11
03:35:40.31	-29:17:08.7	9.0	21.65±0.01	20.26±0.01	19.8±0.05	18.14±0.03	17.62±0.04	17.12±0.07	-	-
03:35:48.51	-29:21:14.7	9.0	21.96±0.02	20.63±0.01	20.28±0.07	18.6±0.05	18.02±0.06	17.63±0.1	17.31±0.1	16.96±0.27
<sup>(1)</sup> 03:36:19.11	-29:24:49.6	7.0	18.44±0.0	17.26±0.0	16.93±0.0	15.38±0.06	14.71±0.07	14.39±0.08	14.19±0.03	13.95±0.03
03:36:24.43	-27:24:31.0	9.0	21.56±0.02	20.2±0.01	19.89±0.05	18.27±0.06	17.55±0.07	17.29±0.1	16.98±0.08	16.81±0.25
03:36:41.95	-26:44:25.6	8.0	22.35±0.03	21.08±0.02	20.86±0.11	19.11±0.15	18.77±0.21	18.21±0.22	-	-
03:37:58.85	-26:59:26.4	8.0	21.5±0.02	20.29±0.01	19.97±0.05	18.29±0.07	17.83±0.09	17.33±0.1	17.02±0.09	17.14
<sup>(1)</sup> 03:38:25.46	-27:26:31.3	7.0	18.19±0.0	17.08±0.0	16.76±0.0	15.25±0.05	14.63±0.06	14.38±0.08	14.09±0.03	13.9±0.03
03:39:11.72	-28:21:14.5	9.0	20.98±0.01	19.62±0.01	19.24±0.03	17.52±0.03	-	-	16.4±0.05	16.06±0.14

**Note:** Objects are listed in the order of RA value. The coordinates are from the DES. SpT indicates the spectral type beginning with M0.0 as 0.0. The object with bold coordinates is the one selected for the spectroscopy observation.

**References.** (1). Sample and SpT. only from Reylé (2018), with *Gaia* coordinates,  $i$ ,  $z$ ,  $Y$  photometry from the DES and  $J$ ,  $H$ ,  $K$  photometry from the 2MASS.

**Table B.2.** 29 L-type UCD candidates as photometric standards in the EDF Fornax and their photometry measurements.

$\alpha$ (hms.ss)	$\delta$ (dms.s)	SpT.	$i$	$z$	$Y$	$J$	$H$	$K$	W1	W2
03:30:26.86	-28:56:38.1	10.0	21.95±0.03	20.45±0.02	20.12±0.07	18.36±0.07	17.68±0.07	17.09±0.07	16.96±0.08	16.91±0.25
03:30:29.06	-27:35:49.7	10.0	22.92±0.08	21.44±0.04	20.92±0.17	19.3±0.11	18.62±0.12	18.31±0.2	17.93±0.16	17.09±0.29
03:30:42.26	-28:40:11.8	10.0	22.93±0.07	21.42±0.03	21.14±0.17	19.18±0.13	18.5±0.14	18.27±0.22	-	-
03:31:13.43	-28:58:15.7	11.0	23.63±0.12	21.99±0.05	21.48±0.17	19.32±0.16	19.01±0.22	-	18.18±0.21	17.73
03:31:16.21	-28:28:17.2	10.0	23.01±0.06	21.61±0.03	21.14±0.2	19.32±0.15	18.61±0.15	18.2±0.2	-	-
03:31:17.74	-26:21:49.0	11.0	22.45±0.05	20.9±0.02	20.54±0.1	18.58±0.06	17.85±0.06	17.45±0.09	16.99±0.08	17.05±0.29
03:31:59.07	-27:39:25.7	10.0	22.48±0.06	21.04±0.03	20.53±0.14	18.79±0.07	18.18±0.08	17.68±0.11	17.52±0.12	16.98±0.26
03:32:46.02	-29:51:00.1	10.0	20.66±0.01	19.18±0.01	18.71±0.02	16.85±0.01	16.25±0.01	15.76±0.02	15.49±0.03	15.19±0.06
03:32:49.43	-26:59:27.1	10.0	22.35±0.04	20.97±0.02	20.56±0.09	18.95±0.08	18.33±0.09	17.99±0.15	17.17±0.09	17.16±0.34
03:32:54.87	-28:02:24.0	10.0	22.91±0.06	21.39±0.03	20.93±0.11	19.11±0.14	18.44±0.13	18.04±0.17	18.22±0.21	17.77
03:33:01.46	-29:31:07.1	10.0	22.07±0.05	20.6±0.03	20.04±0.09	18.22±0.03	17.66±0.04	17.08±0.05	16.8±0.07	16.41±0.16
03:33:21.13	-26:58:40.5	10.0	23.34±0.09	21.64±0.04	21.42±0.18	19.38±0.11	19.03±0.17	18.37±0.21	18.03±0.19	17.66
03:33:27.39	-28:02:53.5	10.0	22.42±0.04	20.95±0.02	20.66±0.09	18.76±0.1	18.28±0.11	17.56±0.11	-	-
03:33:27.77	-28:13:47.5	10.0	23.05±0.07	21.55±0.03	21.03±0.14	19.38±0.17	18.76±0.17	-	18.04±0.17	16.93±0.26
03:33:32.71	-29:25:56.4	11.0	23.51±0.1	21.97±0.05	21.23±0.16	19.48±0.1	19.0±0.13	18.3±0.17	17.97±0.18	17.35
03:33:42.21	-28:09:36.9	10.0	22.5±0.05	21.02±0.02	20.43±0.11	18.79±0.1	18.03±0.09	17.6±0.12	-	-
03:34:03.61	-28:23:31.1	10.0	22.27±0.03	20.82±0.01	20.35±0.07	18.64±0.09	17.77±0.07	17.35±0.09	-	-
03:34:21.25	-28:25:38.2	10.0	22.01±0.03	20.48±0.01	20.09±0.07	18.23±0.06	17.69±0.07	17.26±0.09	17.1±0.08	16.69±0.21
03:34:38.24	-27:18:15.6	10.0	21.36±0.02	19.88±0.01	19.47±0.04	17.62±0.03	17.08±0.03	16.7±0.05	16.31±0.05	15.82±0.1
03:34:55.45	-29:11:16.1	10.0	23.23±0.08	21.81±0.04	21.28±0.21	19.56±0.12	19.14±0.15	-	-	-
03:35:06.87	-27:23:18.1	11.0	21.95±0.02	20.49±0.01	19.96±0.05	18.28±0.06	17.47±0.07	17.03±0.08	16.41±0.05	16.15±0.14
03:35:10.56	-29:16:27.5	10.0	22.87±0.05	21.54±0.03	20.93±0.21	19.29±0.09	18.69±0.1	18.03±0.15	-	-
03:35:22.27	-28:13:39.2	10.0	23.16±0.08	21.58±0.03	21.17±0.17	19.42±0.18	-	-	17.81±0.16	17.26±0.37
03:35:24.78	-27:05:30.0	11.0	21.69±0.02	20.18±0.01	19.76±0.05	17.77±0.05	17.11±0.05	16.54±0.05	16.36±0.05	16.2±0.14
03:35:35.09	-27:30:14.4	11.0	22.36±0.04	21.09±0.02	20.69±0.16	18.79±0.12	18.55±0.18	17.86±0.16	17.05±0.08	16.25±0.15
03:36:35.55	-29:20:43.1	12.0	23.09±0.07	21.78±0.04	21.31±0.18	19.22±0.08	18.52±0.09	18.06±0.15	17.32±0.1	17.75
03:38:00.03	-27:10:18.4	10.0	20.6±0.01	19.14±0.0	18.68±0.02	16.95±0.02	16.34±0.02	15.95±0.03	15.6±0.04	15.31±0.07
03:38:22.29	-27:15:44.0	10.0	20.89±0.01	19.36±0.0	18.91±0.02	17.16±0.02	16.57±0.03	16.17±0.04	15.92±0.04	15.65±0.09
03:38:23.13	-27:41:20.4	10.0	22.23±0.03	20.65±0.01	20.35±0.07	18.43±0.07	17.91±0.11	17.47±0.12	16.79±0.07	16.65±0.23

**Note:** Objects are listed in the order of RA value. The coordinates are from the DES. SpT indicates the spectral type beginning with L0.0 as 10.0. The object with bold coordinates is the one selected for the spectroscopy observation.



## Appendix C: Lists of ultracool dwarf candidates in Euclid Deep Field South

Table C.1. 231 late-M-type UCD candidates as photometric standards in EDF South and their photometry measurements.

$\alpha$ (hhmmss.ss)	$\delta$ (ddmmss.s)	SpT.	$i$	$z$	$Y$	$J$	$H$	$K_s$	W1	W2
03:45:19.13	-48:46:43.8	8.0	21.15±0.01	19.87±0.01	19.6±0.03	17.88±0.04	17.41±0.06	17.01±0.06	16.91±0.06	16.72±0.19
03:45:19.40	-49:58:55.7	9.0	22.09±0.03	20.85±0.01	20.64±0.07	18.82±0.07	18.24±0.09	17.74±0.14	17.56±0.09	18.0
03:45:39.80	-48:50:05.0	8.0	21.84±0.02	20.52±0.01	20.25±0.06	18.49±0.06	18.06±0.1	17.52±0.1	17.39±0.09	17.1±0.25
03:46:06.58	-48:51:15.0	9.0	21.79±0.03	20.38±0.01	19.98±0.05	18.28±0.05	17.73±0.08	17.23±0.08	17.05±0.07	17.21±0.26
03:46:23.36	-50:02:43.4	9.0	22.95±0.08	21.46±0.03	21.17±0.15	19.34±0.11	19.11±0.19	-	-	-
03:47:07.41	-49:57:30.2	8.0	22.81±0.07	21.56±0.03	21.3±0.11	19.61±0.15	19.37±0.24	-	-	-
03:47:19.27	-50:39:19.5	9.0	23.15±0.06	21.87±0.04	21.62±0.2	19.77±0.17	18.96±0.16	18.65±0.28	-	-
03:47:56.08	-49:07:41.8	9.0	21.69±0.03	20.31±0.01	19.89±0.05	18.25±0.05	17.64±0.07	17.15±0.07	17.18±0.08	17.05±0.24
03:48:00.23	-49:13:44.7	9.0	23.17±0.12	21.71±0.05	21.47±0.17	19.68±0.19	-	-	18.33±0.2	17.98
03:48:08.05	-49:42:49.2	9.0	22.82±0.07	21.38±0.03	21.02±0.1	19.19±0.1	19.05±0.18	18.68±0.3	-	-
03:48:29.08	-49:02:36.9	9.0	22.54±0.05	21.1±0.02	20.86±0.12	18.92±0.1	18.54±0.17	18.22±0.2	-	-
03:48:36.29	-49:30:32.3	8.0	20.99±0.01	19.67±0.01	19.37±0.02	17.71±0.03	17.26±0.05	16.84±0.05	16.54±0.05	16.62±0.16
03:48:54.98	-49:36:40.3	9.0	21.91±0.04	20.45±0.02	20.04±0.06	18.29±0.04	17.73±0.06	17.38±0.1	-	-
<sup>(1)</sup> 03:49:17.65	-49:18:44.3	7.0	17.79±0.0	16.68±0.0	16.36±0.0	14.9±0.05	14.4±0.06	13.96±0.05	13.75±0.02	13.5±0.03
03:49:17.82	-48:37:07.9	9.0	22.02±0.03	20.61±0.02	20.3±0.07	18.46±0.07	17.98±0.09	17.57±0.1	-	-
03:49:31.46	-49:33:23.0	9.0	22.64±0.09	21.23±0.03	20.81±0.1	19.16±0.12	18.69±0.19	18.37±0.22	18.1±0.16	17.34±0.31
03:49:32.72	-49:49:07.3	8.0	22.75±0.09	21.43±0.04	21.22±0.19	19.53±0.13	18.82±0.16	-	-	-
03:49:43.07	-50:39:26.7	9.0	22.64±0.07	21.28±0.03	20.91±0.13	19.24±0.1	18.64±0.13	18.29±0.21	-	-
03:50:30.74	-50:11:14.3	8.0	23.08±0.08	21.8±0.04	21.56±0.18	19.84±0.18	19.31±0.23	-	-	-
03:50:52.18	-49:17:27.4	9.0	23.39±0.12	21.88±0.05	21.54±0.16	19.87±0.16	19.39±0.24	-	-	-
03:51:00.79	-48:58:29.1	8.0	21.58±0.02	20.37±0.01	20.13±0.06	18.48±0.07	18.11±0.1	17.71±0.11	-	-
<sup>(1)</sup> 03:51:03.69	-50:12:49.8	7.5	17.84±0.0	16.69±0.0	16.38±0.0	14.85±0.04	14.4±0.05	13.9±0.06	13.76±0.02	13.5±0.03
<sup>(1)</sup> 03:51:11.14	-48:54:54.5	8.0	19.2±0.0	17.8±0.0	17.37±0.01	15.76±0.08	15.05±0.09	14.56±0.09	14.4±0.03	14.24±0.03
03:51:20.26	-49:40:36.4	8.0	22.12±0.03	20.89±0.01	20.73±0.08	18.97±0.08	18.55±0.13	18.39±0.22	18.15±0.16	17.62±0.36
03:51:32.35	-50:44:15.8	9.0	20.99±0.01	19.53±0.01	19.16±0.02	17.36±0.02	16.85±0.03	16.4±0.04	16.04±0.04	15.86±0.08
03:51:42.04	-48:42:57.3	9.0	22.4±0.05	21.1±0.02	20.7±0.09	19.01±0.1	18.41±0.14	18.18±0.16	17.8±0.13	17.33
03:51:43.74	-49:07:56.9	9.0	21.56±0.03	20.27±0.01	20.07±0.05	18.29±0.05	17.82±0.08	17.3±0.07	16.66±0.05	16.36±0.13
03:52:22.15	-48:42:55.2	9.0	20.22±0.01	18.87±0.0	18.53±0.02	16.84±0.02	16.21±0.02	15.84±0.02	15.66±0.04	15.48±0.06
03:52:37.18	-47:49:26.8	8.0	20.4±0.01	19.08±0.0	18.75±0.01	17.06±0.02	16.52±0.02	16.18±0.03	15.89±0.04	15.76±0.08
03:52:45.57	-48:30:28.0	8.0	21.46±0.02	20.14±0.01	19.86±0.05	18.13±0.05	17.64±0.07	17.22±0.07	17.06±0.08	17.15±0.27
03:53:17.53	-48:03:25.7	9.0	21.32±0.02	19.96±0.01	19.58±0.04	17.96±0.04	17.4±0.05	16.98±0.06	16.28±0.04	16.34±0.13
03:53:19.12	-47:58:23.2	9.0	22.83±0.06	21.43±0.03	21.19±0.16	19.24±0.12	19.12±0.25	18.34±0.21	-	-
03:53:20.25	-49:24:58.9	8.0	21.64±0.02	20.29±0.01	20.08±0.04	18.39±0.04	17.93±0.07	17.47±0.09	17.53±0.1	17.27±0.28
<sup>(1)</sup> 03:53:37.60	-48:47:08.3	7.5	18.29±0.0	17.15±0.0	16.54±0.01	15.47±0.07	14.89±0.08	14.43±0.08	13.97±0.03	13.82±0.03
03:53:42.64	-47:52:49.3	9.0	23.11±0.08	21.44±0.02	21.18±0.11	19.44±0.15	18.76±0.17	18.33±0.21	18.27±0.19	17.8
03:53:43.92	-49:41:09.2	8.0	21.22±0.02	19.99±0.01	19.75±0.04	18.06±0.04	17.53±0.05	17.15±0.07	-	-
03:53:48.29	-47:42:39.1	9.0	20.6±0.01	19.22±0.0	18.82±0.01	17.16±0.02	16.56±0.02	16.17±0.03	15.8±0.04	15.47±0.06
03:53:57.63	-49:08:34.9	9.0	22.57±0.04	21.19±0.02	20.89±0.07	19.19±0.08	18.67±0.14	18.24±0.19	-	-
03:54:00.42	-48:58:48.8	7.0	21.34±0.01	20.06±0.01	19.89±0.04	18.17±0.03	17.89±0.07	17.39±0.08	17.4±0.09	17.08±0.25
03:54:04.31	-50:28:02.4	8.0	21.57±0.02	20.21±0.01	20.02±0.05	18.22±0.04	17.78±0.06	17.28±0.08	17.23±0.08	17.28±0.27
03:54:05.57	-47:30:22.9	9.0	19.37±0.0	17.82±0.0	17.38±0.0	15.68±0.01	15.26±0.01	14.84±0.01	14.47±0.03	14.11±0.03
03:54:06.42	-49:20:12.0	9.0	21.32±0.02	20.01±0.01	19.61±0.03	17.91±0.03	17.41±0.04	16.92±0.05	16.66±0.06	16.54±0.15
03:54:13.54	-49:06:26.5	8.0	20.86±0.01	19.65±0.01	19.37±0.03	17.72±0.02	17.28±0.04	16.86±0.05	16.78±0.06	17.0±0.23
03:54:18.94	-49:56:01.8	8.0	22.8±0.06	21.46±0.02	21.27±0.14	19.56±0.14	19.02±0.19	-	-	-
03:54:29.21	-48:22:00.7	9.0	22.02±0.02	20.7±0.01	20.36±0.06	18.54±0.05	18.04±0.07	17.65±0.11	17.83±0.13	17.3±0.28
03:54:37.55	-48:13:17.7	8.0	22.23±0.03	20.96±0.02	20.63±0.08	18.94±0.07	18.36±0.1	17.94±0.14	-	-
03:55:03.14	-49:47:56.9	9.0	19.41±0.0	18.12±0.0	17.77±0.01	16.08±0.01	15.48±0.01	15.05±0.01	14.84±0.03	14.62±0.04
03:55:11.93	-50:00:00.6	8.0	20.82±0.01	19.57±0.0	19.3±0.02	17.69±0.03	17.09±0.03	16.62±0.04	16.57±0.05	16.21±0.11
03:55:15.18	-50:14:53.9	9.0	22.9±0.09	21.54±0.03	21.12±0.12	19.39±0.12	18.68±0.14	18.44±0.22	-	-
03:55:15.55	-47:54:52.5	8.0	21.61±0.02	20.32±0.01	20.12±0.05	18.46±0.06	17.82±0.07	17.44±0.09	17.54±0.1	17.77
<sup>(1)</sup> 03:55:16.15	-48:02:54.4	7.0	18.48±0.0	17.45±0.0	17.15±0.0	15.75±0.07	15.07±0.09	14.63±0.1	14.36±0.03	14.14±0.03
03:55:28.95	-48:32:34.3	8.0	22.31±0.03	20.96±0.01	20.75±0.08	19.15±0.08	18.78±0.15	18.6±0.25	-	-
03:55:31.89	-47:52:54.0	8.0	22.13±0.03	20.9±0.02	20.61±0.08	18.94±0.09	18.32±0.11	18.12±0.17	17.82±0.12	17.7
03:55:35.72	-48:30:12.1	8.0	21.64±0.02	20.42±0.01	20.15±0.05	18.51±0.04	17.98±0.07	17.62±0.1	17.18±0.08	16.9±0.19
03:55:48.40	-48:23:07.8	8.0	22.38±0.04	21.08±0.02	20.88±0.13	19.23±0.08	18.37±0.1	18.33±0.2	17.91±0.14	17.82
03:55:56.12	-50:47:36.6	9.0	22.78±0.09	21.45±0.04	21.05±0.19	19.3±0.11	18.73±0.15	18.76±0.3	-	-
03:56:01.81	-48:50:41.4	8.0	21.56±0.02	20.3±0.01	20.08±0.05	18.43±0.04	17.88±0.06	17.48±0.09	17.26±0.08	17.52±0.34
03:56:02.10	-48:47:25.7	9.0	21.05±0.01	19.71±0.01	19.37±0.04	17.57±0.02	16.99±0.03	16.52±0.04	16.27±0.04	16.16±0.1
03:56:04.15	-50:41:42.3	9.0	20.16±0.01	18.83±0.0	18.48±0.01	16.79±0.01	16.23±0.02	15.81±0.02	15.6±0.03	15.47±0.06
03:56:07.16	-48:28:04.7	8.0	19.73±0.0	18.53±0.0	18.25±0.01	16.59±0.01	16.08±0.01	15.72±0.02	15.46±0.03	15.41±0.06
03:56:20.48	-49:27:49.7	9.0	22.67±0.05	21.27±0.02	20.87±0.09	19.25±0.09	18.7±0.14	18.32±0.2	18.03±0.16	17.65
03:56:28.24	-50:47:56.9	9.0	22.69±0.06	21.47±0.03	20.99±0.14	19.07±0.09	19.4±0.27	18.99±0.37	-	-
03:56:33.13	-50:51:59.4	8.0	21.86±0.04	20.6±0.02	20.32±0.1	18.53±0.05	18.15±0.08	17.65±0.11	17.71±0.11	17.33
03:56:48.54	-50:01:42.3	8.0	22.06±0.05	20.72±0.02	20.54±0.11	18.77±0.06	18.25±0.08	17.65±0.1	17.66±0.11	17.78

Table C.1. continued.

$\alpha$ (hms.ss)	$\delta$ (dms.s)	SpT.	$i$	$z$	$Y$	$J$	$H$	$K_s$	W1	W2
03:56:54.00	-50:01:43.3	8.0	21.39±0.02	20.18±0.01	20.02±0.06	18.33±0.04	17.76±0.05	17.41±0.08	17.29±0.08	16.74±0.18
03:57:08.27	-47:27:26.7	8.0	23.18±0.08	21.76±0.03	21.56±0.14	19.73±0.14	19.65±0.21	18.93±0.28	-	-
03:57:16.28	-47:12:02.4	8.0	22.86±0.06	21.41±0.02	21.17±0.1	19.41±0.1	19.25±0.15	18.67±0.21	-	-
03:57:28.44	-47:34:55.6	9.0	22.47±0.04	21.05±0.02	20.72±0.07	19.02±0.07	18.64±0.08	18.04±0.12	17.77±0.12	17.47
03:57:31.65	-49:19:08.2	8.0	22.79±0.07	21.55±0.04	21.26±0.21	19.59±0.12	19.04±0.2	18.62±0.26	-	-
03:57:37.47	-51:07:22.5	9.0	22.83±0.06	21.38±0.03	21.14±0.12	19.35±0.07	-	18.4±0.18	17.83±0.13	17.8
03:57:47.77	-50:37:49.0	9.0	17.61±0.0	16.2±0.0	15.82±0.0	14.15±0.0	13.62±0.0	13.22±0.0	12.92±0.02	12.66±0.02
03:57:54.66	-48:13:34.0	8.0	21.26±0.01	20.02±0.01	19.63±0.03	18.0±0.03	17.42±0.04	16.96±0.06	16.74±0.06	16.64±0.17
03:57:54.75	-47:17:03.7	8.0	22.67±0.06	21.36±0.03	21.1±0.13	19.48±0.11	18.99±0.12	18.66±0.21	-	-
03:58:00.36	-47:10:34.2	8.0	22.96±0.06	21.61±0.03	21.44±0.15	19.78±0.14	19.47±0.18	18.87±0.26	-	-
03:58:12.63	-51:00:47.8	9.0	22.72±0.05	21.27±0.03	20.86±0.1	19.13±0.08	18.7±0.12	18.11±0.16	-	-
(1)03:58:15.66	-50:26:33.1	7.5	17.62±0.0	16.48±0.0	16.15±0.0	14.69±0.03	14.1±0.04	13.75±0.05	13.56±0.02	13.34±0.03
03:58:32.22	-47:28:14.2	8.0	21.18±0.01	19.84±0.01	19.58±0.03	17.88±0.03	17.32±0.03	16.87±0.04	-	-
03:58:43.85	-49:07:02.0	8.0	19.49±0.0	18.2±0.0	17.86±0.01	16.2±0.01	15.63±0.01	15.19±0.01	14.98±0.03	14.82±0.04
03:58:59.76	-49:20:47.5	9.0	21.21±0.01	19.84±0.01	19.43±0.03	17.78±0.03	17.24±0.04	16.85±0.05	16.36±0.05	15.84±0.08
03:59:00.41	-49:18:51.6	9.0	22.7±0.05	21.31±0.02	20.95±0.11	19.06±0.08	18.67±0.13	18.68±0.26	-	-
03:59:10.96	-50:12:46.7	9.0	21.15±0.01	19.8±0.01	19.42±0.03	17.69±0.02	17.12±0.03	16.69±0.04	16.52±0.05	16.32±0.12
03:59:20.16	-48:07:06.5	9.0	22.85±0.05	21.57±0.02	21.24±0.13	19.46±0.11	18.91±0.11	18.6±0.2	-	-
03:59:21.11	-47:01:42.4	8.0	22.14±0.03	20.88±0.02	20.64±0.06	19.0±0.07	18.51±0.07	17.99±0.12	-	-
03:59:31.49	-47:42:06.4	9.0	23.17±0.06	21.78±0.02	21.52±0.13	19.88±0.16	19.16±0.14	18.77±0.23	-	-
03:59:39.21	-50:05:06.9	8.0	20.78±0.01	19.51±0.01	19.14±0.03	17.54±0.02	16.95±0.02	16.53±0.04	16.42±0.05	15.97±0.09
03:59:42.78	-48:22:00.8	9.0	22.31±0.03	20.93±0.01	20.64±0.06	18.81±0.06	18.05±0.07	17.7±0.11	17.57±0.1	17.35
03:59:44.73	-46:58:13.1	9.0	22.74±0.05	21.24±0.02	20.9±0.08	19.1±0.08	18.62±0.08	18.06±0.12	17.77±0.12	17.76
03:59:51.60	-48:07:54.0	9.0	21.97±0.02	20.51±0.01	20.15±0.04	18.47±0.05	17.92±0.04	17.6±0.08	17.44±0.1	17.06±0.23
03:59:52.37	-50:53:23.5	9.0	22.61±0.05	21.3±0.03	21.04±0.14	19.13±0.08	18.87±0.14	18.33±0.19	17.72±0.11	18.03
03:59:56.49	-49:43:13.4	8.0	23.21±0.08	21.85±0.04	21.49±0.18	19.88±0.16	19.4±0.22	-	-	-
04:00:20.29	-50:22:32.9	9.0	22.5±0.03	21.04±0.02	20.76±0.09	18.89±0.06	18.44±0.09	18.01±0.14	-	-
04:00:20.91	-47:04:50.5	9.0	22.77±0.05	21.44±0.03	21.07±0.14	19.34±0.1	18.85±0.1	18.38±0.16	-	-
04:00:27.73	-47:36:17.3	8.0	23.09±0.04	21.86±0.02	21.53±0.14	19.78±0.15	19.61±0.2	-	-	-
04:00:29.55	-47:42:44.0	8.0	21.05±0.01	19.8±0.01	19.45±0.03	17.84±0.03	17.28±0.03	16.93±0.04	16.81±0.06	17.03±0.24
04:00:31.78	-50:30:07.0	9.0	21.88±0.02	20.49±0.01	20.04±0.05	18.38±0.04	17.68±0.05	17.22±0.07	17.07±0.07	17.46±0.32
04:00:45.34	-49:04:34.3	8.0	20.21±0.01	18.94±0.0	18.63±0.01	16.98±0.01	16.41±0.02	16.03±0.02	15.8±0.04	15.54±0.07
04:00:51.27	-48:30:50.5	9.0	22.46±0.03	21.03±0.01	20.75±0.07	19.01±0.07	18.54±0.12	17.92±0.13	17.65±0.12	17.87
04:00:54.87	-47:40:16.1	8.0	21.29±0.01	20.07±0.01	19.78±0.03	18.17±0.03	17.67±0.04	17.48±0.07	17.04±0.07	16.75±0.18
04:01:10.36	-48:29:41.8	8.0	22.31±0.03	21.04±0.01	20.71±0.06	19.07±0.08	18.46±0.11	17.96±0.14	17.81±0.13	17.66
04:01:13.00	-46:58:46.7	9.0	23.07±0.07	21.51±0.03	21.28±0.1	19.44±0.11	18.89±0.1	18.68±0.22	-	-
04:01:20.78	-48:22:57.1	9.0	22.65±0.03	21.23±0.01	20.96±0.09	19.13±0.09	18.66±0.13	18.48±0.23	-	-
04:01:30.72	-46:53:42.3	9.0	21.65±0.03	20.29±0.01	19.95±0.04	18.33±0.04	17.9±0.04	17.51±0.08	16.93±0.06	16.54±0.14
04:01:43.21	-48:22:35.2	9.0	22.21±0.03	20.82±0.01	20.53±0.06	18.64±0.06	18.16±0.08	17.79±0.12	17.58±0.11	17.21±0.27
04:01:53.22	-47:20:54.5	9.0	22.05±0.02	20.78±0.01	20.33±0.06	18.68±0.05	18.16±0.05	17.67±0.09	17.15±0.07	16.88±0.2
04:01:57.82	-47:37:03.0	8.0	21.54±0.01	20.3±0.01	20.04±0.04	18.39±0.04	17.84±0.04	17.45±0.07	17.51±0.1	17.05±0.22
04:02:21.45	-48:02:19.9	9.0	22.04±0.03	20.67±0.01	20.3±0.05	18.49±0.05	18.07±0.05	17.7±0.09	17.17±0.07	17.06±0.22
04:02:30.92	-49:06:55.8	8.0	21.97±0.03	20.74±0.02	20.49±0.08	18.76±0.06	18.05±0.07	17.63±0.1	17.72±0.11	17.59±0.36
04:02:46.55	-48:44:01.4	8.0	21.25±0.01	19.98±0.01	19.65±0.04	18.0±0.03	17.45±0.04	17.1±0.06	16.84±0.06	17.76
04:02:47.77	-46:42:36.8	9.0	22.75±0.05	21.24±0.02	20.95±0.09	19.06±0.07	18.67±0.09	18.17±0.14	-	-
(1)04:02:56.61	-47:08:07.3	7.0	18.09±0.0	17.07±0.0	16.79±0.0	15.47±0.06	14.8±0.06	14.58±0.09	14.27±0.03	14.06±0.03
04:03:05.97	-48:02:18.1	9.0	23.1±0.05	21.69±0.02	21.45±0.13	19.68±0.11	-	18.52±0.27	-	-
04:03:06.10	-49:28:52.8	8.0	22.94±0.07	21.55±0.03	21.37±0.18	19.62±0.14	19.15±0.21	-	-	-
(1)04:03:31.60	-47:39:35.3	7.0	18.08±0.0	17.09±0.0	16.81±0.0	15.4±0.05	14.78±0.06	14.36±0.07	14.21±0.02	14.07±0.03
04:03:35.25	-49:53:49.0	9.0	21.06±0.01	19.77±0.01	19.45±0.03	17.72±0.04	17.16±0.07	16.75±0.06	16.5±0.05	16.6±0.15
04:03:51.34	-46:47:56.2	8.0	21.17±0.01	19.96±0.01	19.63±0.03	18.01±0.03	-	17.02±0.07	16.94±0.06	16.53±0.14
04:04:06.50	-47:28:52.6	9.0	22.41±0.04	21.04±0.02	20.64±0.08	19.04±0.06	-	17.67±0.12	17.61±0.1	17.84
04:04:19.12	-48:30:43.3	9.0	21.73±0.02	20.31±0.01	19.94±0.04	18.29±0.04	-	17.21±0.1	17.14±0.07	17.31±0.29
04:04:21.56	-50:16:28.9	8.0	20.2±0.01	18.99±0.0	18.69±0.02	17.07±0.02	16.31±0.03	16.15±0.04	15.96±0.04	15.84±0.08
04:04:57.19	-48:12:33.7	9.0	22.3±0.05	20.84±0.02	20.61±0.07	18.73±0.06	-	-	17.62±0.1	17.7±0.39
04:05:02.04	-49:55:19.5	9.0	21.91±0.02	20.57±0.02	20.33±0.08	18.58±0.08	17.83±0.14	17.51±0.13	-	-
04:05:02.60	-49:13:53.1	8.0	22.18±0.04	20.89±0.02	20.57±0.09	18.89±0.08	-	17.94±0.19	-	-
04:05:11.25	-47:06:26.5	8.0	19.97±0.0	18.77±0.0	18.47±0.01	16.81±0.01	-	15.83±0.02	15.66±0.03	15.51±0.06
(1)04:05:13.30	-49:47:21.7	7.0	17.41±0.0	16.4±0.0	16.11±0.0	14.71±0.03	14.21±0.04	13.8±0.05	13.62±0.02	13.41±0.03
04:05:18.33	-48:05:18.1	9.0	22.51±0.04	21.1±0.02	20.94±0.1	19.1±0.07	-	18.48±0.26	-	-
04:05:19.52	-47:07:00.9	8.0	22.46±0.04	21.19±0.02	21.02±0.12	19.17±0.08	-	18.45±0.25	-	-
04:05:26.49	-48:53:55.3	9.0	21.72±0.02	20.32±0.01	20.02±0.05	18.31±0.04	-	17.51±0.13	17.17±0.08	16.92±0.2
04:05:30.15	-48:20:03.0	8.0	22.19±0.03	20.9±0.01	20.63±0.07	19.0±0.09	-	-	-	-
04:05:45.73	-49:58:52.2	8.0	20.76±0.01	19.45±0.0	19.15±0.03	17.47±0.03	16.98±0.07	16.66±0.06	16.35±0.04	16.05±0.1
04:05:52.99	-46:52:19.8	8.0	19.31±0.0	18.09±0.0	17.78±0.01	16.17±0.01	-	15.24±0.01	14.98±0.03	14.75±0.04
04:05:59.62	-46:40:21.9	8.0	22.05±0.03	20.8±0.01	20.62±0.08	18.87±0.05	18.32±0.07	18.03±0.13	17.95±0.13	17.69
04:06:25.84	-50:01:59.4	9.0	22.52±0.04	21.16±0.02	20.85±0.1	19.15±0.08	18.62±0.13	18.06±0.15	18.02±0.15	17.73

Table C.1. continued.

$\alpha$ (hms.ss)	$\delta$ (dms.s)	SpT.	$i$	$z$	$Y$	$J$	$H$	$K_s$	W1	W2
04:06:30.80	-47:14:18.7	8.0	22.21±0.03	20.88±0.02	20.69±0.09	18.93±0.05	-	17.85±0.13	17.85±0.12	18.1
04:06:31.18	-48:33:41.2	8.0	21.8±0.02	20.43±0.01	20.07±0.05	18.39±0.03	-	17.52±0.1	17.28±0.08	17.39±0.29
04:06:31.35	-47:08:53.0	9.0	22.55±0.04	21.3±0.02	20.92±0.11	19.21±0.07	-	18.27±0.19	17.96±0.14	17.36
<sup>(1)</sup> 04:06:32.11	-47:11:34.5	7.0	17.82±0.0	16.72±0.0	16.41±0.0	14.98±0.03	14.32±0.02	14.01±0.06	13.76±0.02	13.56±0.03
04:06:51.93	-48:12:37.0	9.0	22.76±0.06	21.49±0.03	21.06±0.11	19.43±0.09	-	18.43±0.23	-	-
04:06:59.62	-49:12:03.0	8.0	21.93±0.03	20.66±0.01	20.44±0.09	18.74±0.05	-	17.75±0.13	17.92±0.13	17.61
04:07:27.25	-48:29:01.9	8.0	22.61±0.05	21.41±0.02	21.14±0.13	19.36±0.08	-	18.5±0.25	18.12±0.16	17.77
04:07:30.03	-48:16:05.1	9.0	22.77±0.05	21.36±0.03	21.19±0.12	19.26±0.07	-	18.38±0.21	18.2±0.16	17.46
04:07:37.91	-48:57:15.1	8.0	21.25±0.02	19.88±0.01	19.58±0.05	17.87±0.02	-	16.94±0.05	16.71±0.05	16.61±0.14
04:07:39.06	-46:55:23.0	8.0	21.88±0.02	20.63±0.01	20.39±0.07	18.71±0.05	-	17.84±0.13	17.72±0.11	17.96
04:07:42.28	-46:20:55.1	9.0	21.71±0.02	20.37±0.01	20.16±0.09	18.38±0.05	17.75±0.07	17.28±0.08	17.13±0.07	17.16±0.23
04:07:42.83	-46:16:47.2	9.0	23.06±0.08	21.71±0.05	21.37±0.21	19.76±0.17	19.39±0.3	18.47±0.22	18.45±0.2	17.45
04:07:48.40	-49:36:24.7	8.0	22.64±0.06	21.35±0.03	21.09±0.17	19.36±0.1	19.35±0.26	18.72±0.28	-	-
04:08:07.82	-46:48:44.5	8.0	20.73±0.01	19.51±0.01	19.22±0.03	17.6±0.02	-	16.58±0.04	16.43±0.05	16.26±0.11
04:09:31.20	-48:45:52.9	9.0	19.99±0.01	18.58±0.0	18.21±0.01	16.42±0.01	-	15.34±0.02	15.1±0.03	14.89±0.04
<sup>(1)</sup> 04:09:51.06	-49:46:03.2	7.0	18.0±0.0	16.94±0.0	16.64±0.0	15.17±0.05	14.58±0.06	14.28±0.06	14.05±0.03	13.84±0.03
04:10:15.56	-48:01:17.3	8.0	21.9±0.02	20.65±0.01	20.34±0.07	18.7±0.04	-	17.72±0.11	17.48±0.09	17.39
04:10:16.59	-49:48:42.3	9.0	22.18±0.03	20.82±0.01	20.41±0.07	18.73±0.06	18.26±0.09	17.68±0.11	-	-
04:10:16.63	-46:20:33.8	9.0	21.68±0.02	20.2±0.01	19.9±0.06	18.02±0.03	17.48±0.05	17.13±0.06	16.73±0.05	16.5±0.13
04:10:16.91	-46:16:05.6	9.0	21.34±0.01	19.85±0.01	19.59±0.05	17.73±0.03	17.15±0.04	16.72±0.05	16.4±0.04	16.26±0.1
04:10:28.54	-48:13:03.5	9.0	21.66±0.02	20.24±0.01	20.06±0.05	18.21±0.03	-	17.29±0.08	17.17±0.07	16.66±0.16
04:10:30.18	-47:20:26.6	8.0	20.54±0.01	19.28±0.01	18.96±0.03	17.35±0.01	-	16.48±0.04	16.18±0.04	16.77±0.16
04:10:55.93	-48:12:33.9	8.0	22.4±0.04	21.17±0.02	21.01±0.1	19.09±0.06	-	18.49±0.22	17.91±0.12	17.91
04:11:10.25	-48:52:36.8	8.0	21.05±0.01	19.76±0.01	19.56±0.03	17.82±0.02	-	16.87±0.05	16.68±0.05	16.59±0.14
04:11:26.84	-47:08:56.7	9.0	22.79±0.05	21.42±0.03	21.16±0.13	19.48±0.1	-	18.18±0.18	18.44±0.2	17.59
04:11:27.67	-47:51:00.6	8.0	21.74±0.02	20.4±0.01	20.17±0.07	18.43±0.04	-	17.46±0.09	17.3±0.08	16.97±0.2
04:11:38.51	-47:55:58.7	9.0	22.77±0.07	21.5±0.03	21.24±0.18	19.5±0.11	-	18.28±0.2	-	-
04:11:39.42	-46:07:07.9	9.0	23.07±0.2	21.57±0.04	21.35±0.21	19.49±0.08	18.81±0.1	18.67±0.23	-	-
04:11:41.41	-47:37:12.7	9.0	22.93±0.06	21.45±0.03	21.29±0.13	19.29±0.09	-	18.21±0.19	18.45±0.2	17.46
04:11:44.10	-46:37:29.8	9.0	22.49±0.04	21.13±0.03	20.97±0.11	19.14±0.06	18.44±0.07	17.99±0.13	-	-
04:11:45.49	-46:16:39.1	9.0	22.3±0.03	20.77±0.02	20.43±0.1	18.62±0.04	18.06±0.05	17.55±0.08	17.61±0.1	17.4
<sup>(1)</sup> 04:11:55.13	-48:55:57.1	7.0	18.54±0.0	17.43±0.0	17.11±0.0	15.69±0.07	15.1±0.09	14.77±0.1	14.35±0.03	14.15±0.03
04:12:19.58	-49:25:11.0	8.0	19.56±0.0	18.33±0.0	18.04±0.01	16.43±0.01	-	15.42±0.02	15.07±0.03	14.82±0.04
04:12:20.77	-49:27:19.6	9.0	22.11±0.03	20.75±0.01	20.37±0.08	18.77±0.05	-	17.8±0.13	17.37±0.08	17.5±0.31
04:12:27.17	-46:30:03.2	9.0	21.96±0.02	20.6±0.01	20.27±0.06	18.45±0.03	17.84±0.04	17.41±0.07	-	-
04:12:57.88	-49:17:39.2	9.0	21.66±0.01	20.33±0.01	19.93±0.05	18.23±0.04	-	17.13±0.08	-	-
04:12:58.78	-45:55:07.7	9.0	21.24±0.01	19.92±0.01	19.67±0.05	17.89±0.02	17.31±0.03	16.84±0.04	16.69±0.05	16.45±0.14
04:13:00.78	-46:43:52.8	8.0	21.32±0.01	20.09±0.01	19.83±0.05	18.19±0.03	-	17.29±0.08	17.22±0.07	16.82±0.18
04:13:01.66	-49:23:53.9	8.0	21.34±0.02	19.99±0.01	19.69±0.04	18.02±0.03	-	16.98±0.07	16.83±0.05	16.69±0.15
04:13:12.58	-48:43:18.5	9.0	22.16±0.03	20.96±0.02	20.52±0.07	18.92±0.07	-	18.01±0.18	17.34±0.08	17.17±0.23
04:13:13.94	-46:16:39.3	8.0	22.84±0.06	21.59±0.04	21.2±0.18	19.55±0.08	19.01±0.11	18.67±0.23	-	-
04:13:18.15	-47:35:42.2	8.0	22.61±0.06	21.14±0.03	20.77±0.11	19.1±0.07	-	18.34±0.21	18.33±0.18	17.38
04:13:36.73	-46:57:28.4	8.0	22.06±0.03	20.75±0.02	20.56±0.08	18.81±0.06	-	17.7±0.12	-	-
04:13:42.64	-45:53:42.1	9.0	23.11±0.08	21.58±0.04	21.18±0.18	19.57±0.09	18.87±0.1	18.46±0.19	18.33±0.2	17.84
04:13:44.66	-48:26:33.9	9.0	22.44±0.04	21.06±0.02	20.7±0.1	18.92±0.07	-	17.88±0.15	-	-
04:13:56.62	-47:45:02.6	9.0	22.63±0.05	21.4±0.03	21.08±0.15	19.44±0.1	-	18.43±0.23	18.0±0.13	17.79
04:14:00.85	-48:34:29.6	8.0	20.02±0.0	18.77±0.0	18.49±0.02	16.82±0.01	-	15.91±0.03	15.74±0.03	15.54±0.06
04:14:06.02	-46:20:50.2	9.0	21.78±0.02	20.54±0.02	20.24±0.07	18.55±0.04	17.88±0.04	17.41±0.07	17.33±0.09	16.95±0.2
04:14:15.86	-47:50:23.0	9.0	21.54±0.02	20.19±0.01	19.86±0.05	18.18±0.03	-	17.24±0.08	-	-
04:14:23.58	-46:44:39.1	7.0	20.54±0.01	19.28±0.01	19.07±0.02	17.44±0.02	-	16.64±0.05	16.46±0.05	16.44±0.13
04:14:34.28	-47:47:02.0	9.0	19.82±0.01	18.53±0.0	18.13±0.01	16.46±0.01	-	15.49±0.02	15.26±0.03	15.1±0.05
04:14:50.51	-46:31:26.7	8.0	22.87±0.06	21.57±0.04	21.32±0.2	19.48±0.08	19.19±0.13	18.59±0.22	-	-
04:14:51.30	-48:38:21.5	8.0	22.04±0.03	20.8±0.02	20.56±0.11	18.91±0.07	-	18.01±0.18	18.01±0.13	17.52
04:15:01.43	-49:29:09.7	9.0	21.33±0.01	19.84±0.01	19.53±0.03	17.74±0.03	-	16.77±0.06	16.56±0.05	15.97±0.08
04:15:09.21	-49:24:09.1	9.0	21.44±0.02	19.99±0.01	19.61±0.03	18.0±0.03	-	17.04±0.07	16.77±0.05	16.39±0.12
<sup>(1)</sup> 04:15:09.23	-48:53:21.3	sdM7.5	18.81±0.0	17.6±0.0	17.24±0.0	15.96±0.1	15.12±0.08	14.63±0.09	14.45±0.03	14.23±0.03
04:15:16.22	-47:05:57.5	8.0	21.53±0.02	20.31±0.01	19.97±0.05	18.29±0.04	-	17.36±0.09	17.16±0.07	16.69±0.16
04:15:29.52	-46:29:51.5	9.0	22.65±0.05	21.4±0.04	21.04±0.14	19.31±0.07	18.69±0.09	18.43±0.19	-	-
04:15:32.62	-47:57:51.0	8.0	21.46±0.02	20.09±0.01	19.74±0.04	18.12±0.03	-	17.35±0.08	16.96±0.06	16.9±0.18
04:15:41.20	-46:28:17.9	8.0	22.41±0.04	21.11±0.02	20.77±0.1	19.02±0.05	18.8±0.09	18.09±0.14	-	-
04:15:41.73	-46:50:53.3	8.0	22.27±0.03	21.02±0.02	20.68±0.08	19.06±0.07	-	18.1±0.17	17.95±0.14	17.58±0.38
04:15:55.70	-49:31:21.2	8.0	21.19±0.01	19.89±0.01	19.62±0.03	17.86±0.03	-	16.95±0.07	16.69±0.05	16.76±0.15
04:16:00.72	-48:56:44.0	8.0	21.17±0.01	19.9±0.01	19.66±0.04	17.95±0.03	-	17.1±0.08	16.99±0.06	17.46±0.3
04:16:13.71	-46:26:40.8	8.0	21.39±0.02	20.1±0.01	19.74±0.05	18.1±0.02	17.62±0.03	17.16±0.06	-	-
04:16:39.00	-47:45:45.4	8.0	19.68±0.0	18.35±0.0	18.05±0.01	16.44±0.01	-	15.6±0.02	15.36±0.03	15.04±0.04
04:16:48.41	-46:17:11.8	8.0	21.88±0.03	20.52±0.02	20.27±0.09	18.64±0.04	18.17±0.05	17.78±0.1	17.28±0.09	16.87±0.21
04:16:57.36	-49:01:04.1	9.0	20.55±0.01	19.23±0.0	18.87±0.02	17.22±0.02	-	16.18±0.03	16.01±0.04	15.87±0.07

Table C.1. continued.

$\alpha$ (hms.ss)	$\delta$ (dms.s)	SpT.	$i$	$z$	$Y$	$J$	$H$	$K_s$	W1	W2
04:17:00.69	-46:51:51.8	9.0	21.13±0.01	19.69±0.01	19.25±0.03	17.63±0.02	-	16.76±0.05	16.31±0.04	16.01±0.1
04:17:41.38	-46:51:33.8	9.0	22.24±0.03	20.91±0.02	20.63±0.07	18.96±0.07	-	18.15±0.17	17.6±0.1	17.04±0.22
04:17:50.66	-49:09:31.9	8.0	22.86±0.07	21.66±0.04	21.28±0.18	19.61±0.07	-	18.87±0.27	-	-
04:18:02.04	-47:18:35.6	9.0	22.74±0.07	21.23±0.03	20.98±0.14	19.35±0.1	-	18.24±0.19	18.13±0.16	17.96
04:18:04.82	-47:58:09.7	9.0	19.97±0.0	18.61±0.0	18.26±0.01	16.56±0.01	-	15.57±0.02	15.27±0.03	15.14±0.05
04:18:10.41	-48:27:15.0	8.0	22.5±0.04	21.22±0.02	20.86±0.1	19.26±0.05	-	18.15±0.14	18.29±0.17	18.12
<sup>(1)</sup> 04:18:16.75	-48:55:51.4	7.0	16.67±0.0	15.74±0.0	15.31±0.0	13.87±0.03	13.28±0.03	12.91±0.03	12.74±0.02	12.48±0.02
<sup>(1)</sup> 04:18:23.44	-47:05:24.3	7.0	17.45±0.0	16.39±0.0	16.08±0.0	14.6±0.04	14.0±0.04	13.63±0.04	13.36±0.02	13.13±0.03
04:18:33.78	-48:02:23.2	9.0	22.11±0.03	20.79±0.02	20.42±0.07	18.82±0.06	-	17.8±0.12	17.41±0.08	17.01±0.21
04:18:34.08	-46:39:34.4	9.0	22.97±0.07	21.54±0.03	21.36±0.14	19.56±0.19	18.8±0.18	18.73±0.31	-	-
<sup>(1)</sup> 04:18:59.53	-46:45:45.1	7.0	18.34±0.0	17.33±0.0	17.05±0.0	15.6±0.05	15.04±0.07	14.73±0.1	14.5±0.03	14.29±0.03
04:19:08.63	-48:22:34.4	8.0	20.59±0.01	19.34±0.0	19.05±0.02	17.36±0.01	-	16.5±0.03	-	-
04:19:15.36	-48:46:42.3	9.0	21.83±0.03	20.48±0.01	20.04±0.06	18.4±0.03	-	17.45±0.07	17.28±0.07	17.76
04:19:15.76	-48:59:21.1	9.0	22.13±0.03	20.72±0.01	20.44±0.07	18.7±0.03	-	17.67±0.09	17.45±0.08	17.2±0.24
04:19:18.83	-47:15:08.4	9.0	22.85±0.06	21.5±0.04	21.17±0.16	19.54±0.12	-	18.51±0.24	-	-
04:19:46.77	-49:07:15.4	9.0	22.29±0.06	20.96±0.03	20.69±0.13	18.89±0.04	-	17.89±0.11	17.73±0.1	17.38
04:19:56.79	-46:55:56.4	9.0	22.56±0.05	21.34±0.03	21.03±0.15	19.23±0.09	-	18.01±0.15	17.83±0.12	17.85
04:20:08.57	-46:03:29.7	8.0	21.14±0.02	19.82±0.01	19.5±0.05	17.79±0.04	17.22±0.04	16.88±0.06	16.79±0.06	16.57±0.15
04:20:16.30	-46:10:16.4	8.0	21.09±0.01	19.86±0.01	19.57±0.04	17.92±0.04	17.49±0.05	17.11±0.07	-	-
04:20:38.99	-47:12:46.6	8.0	22.36±0.05	20.97±0.03	20.66±0.09	19.05±0.07	-	18.31±0.2	-	-
04:20:44.67	-47:33:12.3	8.0	21.54±0.02	20.21±0.01	19.87±0.04	18.2±0.03	-	17.29±0.08	17.08±0.07	16.8±0.18
04:21:12.80	-48:08:26.1	9.0	21.37±0.01	20.11±0.01	19.82±0.04	18.18±0.02	-	17.25±0.06	16.66±0.05	16.69±0.17
04:21:19.41	-47:58:42.8	8.0	21.59±0.02	20.33±0.01	20.04±0.05	18.33±0.04	-	17.36±0.08	-	-
04:21:28.17	-47:19:03.9	9.0	23.08±0.06	21.63±0.04	21.41±0.15	19.71±0.14	-	18.5±0.24	-	-
04:22:00.67	-47:20:28.6	9.0	21.3±0.01	19.83±0.01	19.5±0.03	17.68±0.02	-	16.69±0.04	16.48±0.05	16.32±0.12
04:22:14.34	-47:55:07.9	9.0	23.2±0.06	21.7±0.03	21.52±0.19	19.89±0.1	-	18.5±0.2	18.03±0.15	17.98
04:22:35.47	-46:39:54.3	9.0	21.97±0.03	20.57±0.02	20.19±0.07	18.49±0.07	17.94±0.08	17.53±0.1	17.18±0.08	16.92±0.2
<sup>(1)</sup> 04:23:22.29	-47:09:45.9	7.5	17.65±0.0	16.54±0.0	16.23±0.0	14.76±0.04	14.16±0.04	13.81±0.05	13.56±0.02	13.32±0.03
<sup>(1)</sup> 04:23:25.03	-47:03:54.8	7.5	17.3±0.0	16.11±0.0	15.77±0.0	14.24±0.03	13.64±0.03	13.29±0.04	13.05±0.02	12.82±0.02
04:23:59.21	-46:58:46.2	8.0	22.66±0.05	21.4±0.03	21.18±0.16	19.49±0.07	-	18.51±0.21	-	-
<sup>(1)</sup> 04:24:32.14	-47:25:25.7	7.5	18.56±0.0	17.44±0.0	17.14±0.0	15.61±0.06	15.05±0.07	14.83±0.09	14.5±0.03	14.34±0.04
04:24:52.54	-47:19:30.4	9.0	23.16±0.07	21.74±0.04	21.54±0.15	19.84±0.1	-	18.69±0.24	-	-
04:25:02.61	-47:11:47.1	9.0	22.58±0.05	21.25±0.03	21.05±0.13	19.22±0.06	-	18.25±0.16	-	-

**Note:** Objects are listed in the order of RA value. The coordinates are from the DES. The object with bold coordinates is the one selected for the spectroscopy observation.

**References.** (1). Sample and SpT. only from Reylé (2018), with *Gaia* coordinates,  $i$ ,  $z$ ,  $Y$  photometry from the DES and  $J$ ,  $H$ ,  $K$  photometry from the 2MASS.

**Table C.2.** 115 L-type UCD candidates as photometric standards in EDF South and their photometry measurements.

$\alpha$ (hhmmss.ss)	$\delta$ (ddmms.ss)	SpT.	$i$	$z$	$Y$	$J$	$H$	$K_s$	$W1$	$W2$
03:45:35.98	-49:07:26.6	10.0	23.0±0.1	21.39±0.04	21.13±0.19	19.31±0.13	18.61±0.17	18.28±0.19	-	-
03:45:39.39	-49:34:32.7	12.0	22.32±0.06	20.58±0.02	20.1±0.07	17.99±0.04	17.38±0.06	16.97±0.06	16.48±0.05	16.14±0.1
03:46:38.59	-48:37:16.4	10.0	21.52±0.03	19.89±0.01	19.46±0.04	17.63±0.03	17.08±0.04	16.68±0.05	16.44±0.05	16.1±0.11
03:49:04.31	-49:35:41.9	11.0	22.74±0.07	21.28±0.03	20.87±0.08	18.86±0.09	18.28±0.13	17.49±0.1	17.3±0.08	17.56±0.36
03:49:20.90	-49:53:58.3	10.0	20.72±0.01	19.26±0.01	18.79±0.02	16.97±0.01	16.34±0.02	15.92±0.03	15.58±0.03	15.54±0.07
03:49:41.70	-50:30:46.0	13.0	22.27±0.05	20.46±0.02	19.96±0.06	17.82±0.03	17.07±0.03	16.61±0.05	16.0±0.04	15.72±0.07
<b>03:50:25.77</b>	<b>-49:32:20.7</b>	16.0	22.62±0.05	20.72±0.02	20.17±0.05	17.96±0.04	16.98±0.04	16.28±0.03	15.55±0.03	15.24±0.06
03:50:50.36	-50:21:39.0	10.0	21.65±0.02	20.16±0.01	19.71±0.04	17.96±0.03	17.35±0.04	16.95±0.07	16.59±0.05	16.41±0.12
03:51:17.50	-49:36:37.8	10.0	22.73±0.06	21.16±0.02	20.87±0.09	19.0±0.09	18.39±0.11	18.13±0.17	17.29±0.08	16.94±0.21
03:52:03.88	-50:39:22.0	10.0	23.03±0.08	21.52±0.03	21.2±0.12	19.44±0.12	18.55±0.13	18.44±0.23	-	-
03:52:25.33	-50:54:36.5	10.0	21.03±0.01	19.48±0.0	19.07±0.02	17.2±0.02	16.67±0.02	16.29±0.03	15.95±0.04	15.64±0.07
03:52:51.51	-50:51:15.3	10.0	22.29±0.06	20.79±0.02	20.44±0.07	18.41±0.05	17.87±0.07	17.43±0.09	17.22±0.08	16.82±0.18
03:54:33.04	-47:25:35.6	10.0	23.3±0.07	21.75±0.02	21.31±0.14	19.56±0.16	19.0±0.21	18.47±0.23	-	-
03:54:33.28	-49:00:54.2	10.0	22.69±0.05	21.18±0.02	20.86±0.09	18.91±0.06	18.2±0.09	17.74±0.12	17.48±0.1	17.95
03:55:14.48	-47:22:30.8	10.0	23.41±0.1	22.0±0.05	21.44±0.13	19.61±0.17	18.96±0.22	18.62±0.26	-	-
03:55:21.45	-49:40:31.7	10.0	23.31±0.1	21.89±0.03	21.45±0.16	19.64±0.15	18.93±0.18	-	-	-
03:55:37.34	-49:02:26.0	10.0	22.43±0.05	20.95±0.02	20.51±0.07	18.69±0.05	18.04±0.08	17.69±0.11	-	-
03:55:54.12	-49:10:08.9	12.0	22.8±0.06	21.37±0.02	20.78±0.07	18.83±0.06	18.18±0.08	17.51±0.09	-	-
03:56:03.59	-49:44:02.4	10.0	22.51±0.04	21.0±0.01	20.75±0.07	18.84±0.06	18.26±0.08	17.6±0.1	17.39±0.09	16.96±0.22
03:57:29.97	-47:47:35.7	14.0	22.58±0.04	20.85±0.01	20.55±0.07	18.31±0.04	17.43±0.03	16.69±0.04	15.91±0.04	15.8±0.08
03:57:51.75	-48:38:35.8	12.0	22.21±0.03	20.83±0.01	20.42±0.06	18.26±0.04	17.55±0.05	16.87±0.05	16.43±0.05	16.38±0.13
03:57:54.91	-47:07:46.5	10.0	22.58±0.04	21.1±0.02	20.72±0.07	19.0±0.07	18.43±0.07	17.82±0.1	17.72±0.12	17.14±0.25
03:58:26.54	-49:24:50.5	10.0	22.95±0.08	21.54±0.03	21.05±0.12	19.37±0.11	18.58±0.12	18.03±0.15	18.17±0.17	18.04
03:58:39.96	-50:08:03.6	10.0	23.03±0.07	21.59±0.03	21.34±0.18	19.34±0.1	18.8±0.13	18.55±0.23	-	-
03:59:00.45	-49:50:43.4	12.0	23.51±0.1	21.87±0.04	21.29±0.18	19.35±0.1	18.58±0.11	18.11±0.16	-	-
03:59:07.76	-47:13:05.1	10.0	23.07±0.08	21.72±0.03	21.32±0.17	19.46±0.11	18.98±0.11	18.73±0.23	18.0±0.15	17.99
03:59:13.06	-50:36:15.8	12.0	23.24±0.05	21.67±0.02	21.06±0.12	19.3±0.09	18.54±0.1	18.07±0.15	17.04±0.07	17.18±0.26
03:59:24.72	-50:45:11.1	10.0	23.05±0.06	21.5±0.03	21.24±0.13	19.28±0.09	18.73±0.12	18.28±0.18	18.42±0.2	17.32
03:59:53.90	-47:46:03.0	11.0	21.56±0.02	20.03±0.01	19.61±0.03	17.7±0.02	17.01±0.02	16.54±0.03	16.18±0.04	15.85±0.09
04:00:02.36	-50:30:29.8	11.0	23.08±0.07	21.44±0.03	21.2±0.16	19.12±0.08	18.42±0.09	17.89±0.12	17.41±0.09	17.25±0.27
<b>04:00:08.99</b>	<b>-50:50:14.4</b>	16.0	22.85±0.07	20.99±0.03	20.39±0.08	17.94±0.03	17.17±0.03	16.48±0.04	15.86±0.04	15.39±0.06
04:00:37.40	-50:52:23.5	10.0	21.98±0.03	20.52±0.01	20.12±0.06	18.25±0.04	17.57±0.04	17.08±0.06	16.82±0.06	16.48±0.13
04:01:08.86	-47:31:37.2	12.0	23.44±0.05	21.89±0.02	21.35±0.1	19.34±0.09	18.65±0.08	18.18±0.14	17.46±0.09	17.73
04:01:24.69	-46:55:42.8	14.0	22.55±0.05	20.91±0.02	20.51±0.06	18.13±0.03	17.26±0.02	16.56±0.03	15.99±0.04	15.67±0.07
04:01:24.71	-48:50:16.2	12.0	23.05±0.07	21.48±0.02	21.09±0.09	19.01±0.08	18.19±0.09	17.81±0.12	17.29±0.08	17.53±0.34
04:01:37.70	-50:45:22.2	11.0	22.2±0.03	20.82±0.02	20.5±0.07	18.51±0.05	17.79±0.05	17.19±0.07	16.65±0.05	16.41±0.13
04:02:01.35	-48:29:38.3	11.0	22.35±0.03	20.75±0.01	20.44±0.06	18.37±0.04	17.78±0.06	17.25±0.07	-	-
04:02:08.74	-49:45:45.9	13.0	22.59±0.05	21.14±0.02	20.73±0.1	18.61±0.08	17.54±0.11	17.24±0.1	16.52±0.05	16.16±0.1
04:02:24.36	-49:47:56.5	10.0	23.24±0.07	21.75±0.03	21.44±0.18	19.47±0.17	-	-	-	-
04:02:54.77	-49:00:48.5	10.0	22.55±0.04	21.15±0.02	20.98±0.1	18.94±0.07	18.62±0.13	17.85±0.12	17.37±0.09	17.32±0.28
<b>04:02:54.86</b>	<b>-47:04:40.9</b>	15.0	23.63±0.14	21.43±0.03	20.92±0.09	18.91±0.06	-	17.32±0.09	16.53±0.05	16.22±0.11
04:03:08.68	-48:09:40.6	10.0	22.36±0.07	20.89±0.03	20.6±0.1	18.78±0.06	18.16±0.09	17.77±0.12	17.18±0.08	17.43±0.33
04:03:23.90	-48:52:33.2	11.0	22.11±0.03	20.78±0.01	20.38±0.06	18.76±0.06	-	17.55±0.13	16.81±0.06	16.3±0.12
04:03:49.02	-47:24:27.8	12.0	22.65±0.05	21.11±0.02	20.58±0.08	18.59±0.04	-	17.37±0.09	16.58±0.05	16.72±0.16
04:03:49.61	-49:58:13.3	11.0	20.68±0.01	19.17±0.0	18.74±0.02	16.7±0.01	16.02±0.03	15.56±0.02	15.24±0.03	15.04±0.05
04:04:10.67	-47:17:13.2	10.0	22.47±0.04	20.93±0.02	20.42±0.07	18.72±0.05	-	17.46±0.1	-	-
04:04:19.82	-49:40:53.2	10.0	23.0±0.08	21.55±0.03	21.12±0.14	19.51±0.18	-	18.61±0.34	17.81±0.12	17.65±0.38
04:04:27.68	-49:01:01.4	10.0	21.51±0.02	20.07±0.01	19.66±0.03	17.84±0.03	-	16.79±0.07	16.51±0.05	16.24±0.11
04:04:56.54	-49:32:46.4	12.0	23.29±0.08	21.84±0.03	21.49±0.16	19.46±0.15	-	17.83±0.18	17.64±0.11	16.87±0.19
04:05:18.09	-47:32:56.0	10.0	23.5±0.12	21.83±0.03	21.32±0.17	19.55±0.1	-	18.54±0.27	-	-
04:05:20.48	-47:21:05.9	14.0	22.89±0.06	21.2±0.02	20.87±0.09	18.36±0.03	-	16.86±0.06	16.43±0.04	16.1±0.1
04:05:43.26	-46:56:33.1	11.0	22.65±0.04	21.11±0.02	20.66±0.08	18.69±0.05	-	17.72±0.13	-	-
04:06:07.68	-48:44:34.3	10.0	22.72±0.06	21.22±0.03	20.9±0.11	19.03±0.1	-	-	17.67±0.1	17.26±0.26
04:06:11.46	-47:01:37.3	12.0	22.57±0.04	21.04±0.02	20.7±0.1	18.65±0.04	-	17.53±0.1	16.87±0.06	16.42±0.13
04:06:14.28	-48:46:57.4	13.0	23.66±0.26	21.76±0.05	21.41±0.2	19.16±0.11	-	-	17.09±0.07	17.05±0.22
04:06:14.98	-46:33:37.2	10.0	23.31±0.09	21.79±0.05	21.64±0.19	19.58±0.1	18.99±0.13	18.93±0.31	18.56±0.22	17.69
04:06:24.37	-47:57:56.5	10.0	21.96±0.07	20.5±0.01	19.96±0.05	18.19±0.03	-	17.1±0.07	-	-
04:06:24.39	-49:08:32.7	11.0	21.3±0.01	19.81±0.01	19.39±0.03	17.38±0.02	-	16.17±0.04	15.99±0.04	15.81±0.08
04:06:42.31	-49:14:33.5	10.0	22.83±0.06	21.39±0.02	20.9±0.11	19.03±0.08	-	-	17.97±0.14	17.38
04:07:12.50	-46:30:31.6	10.0	23.12±0.08	21.68±0.04	21.32±0.15	19.4±0.12	19.0±0.22	18.46±0.22	-	-
04:07:16.55	-50:01:34.9	13.0	23.0±0.08	21.11±0.02	20.76±0.11	18.57±0.05	17.86±0.07	17.39±0.08	16.79±0.06	16.66±0.15
04:07:27.52	-48:36:57.4	14.0	22.84±0.07	21.16±0.02	20.86±0.1	18.46±0.04	-	17.01±0.06	16.44±0.04	16.04±0.09
04:07:44.52	-49:57:00.2	10.0	21.26±0.02	19.68±0.01	19.3±0.03	17.32±0.02	16.77±0.03	16.31±0.03	16.07±0.04	15.66±0.07
04:07:46.75	-49:05:41.0	11.0	20.99±0.01	19.56±0.01	19.14±0.03	17.23±0.01	-	15.96±0.03	15.69±0.03	15.62±0.06
04:07:48.40	-47:06:50.0	12.0	23.0±0.07	21.7±0.04	21.44±0.16	19.09±0.06	-	17.51±0.09	17.19±0.07	16.94±0.2
04:08:00.93	-49:43:22.1	10.0	21.64±0.02	20.15±0.01	19.81±0.04	18.02±0.03	17.3±0.04	16.84±0.05	16.65±0.05	16.59±0.15
04:08:03.81	-48:28:31.2	11.0	22.65±0.04	21.13±0.02	20.75±0.1	18.7±0.04	-	17.58±0.1	17.41±0.09	16.53±0.13



Table C.2. continued.

$\alpha$ (hms.ss)	$\delta$ (dms.s)	SpT.	$i$	$z$	$Y$	$J$	$H$	$K_s$	W1	W2
04:08:36.28	-46:53:09.8	10.0	22.37±0.04	20.88±0.02	20.37±0.1	18.72±0.05	-	17.51±0.1	17.31±0.08	17.02±0.21
04:09:24.48	-48:07:57.2	11.0	23.39±0.12	21.86±0.04	21.33±0.19	19.41±0.08	-	18.48±0.22	18.26±0.17	17.16±0.23
04:09:47.62	-49:00:48.2	10.0	22.71±0.04	21.32±0.02	20.76±0.13	19.15±0.07	-	18.01±0.15	-	-
04:09:52.00	-46:38:10.2	10.0	22.88±0.05	21.34±0.02	20.91±0.16	19.3±0.11	18.53±0.14	18.34±0.19	-	-
04:10:03.66	-48:53:38.0	11.0	22.85±0.06	21.63±0.03	20.77±0.17	19.05±0.06	-	17.92±0.13	-	-
04:10:18.84	-49:34:50.4	10.0	23.05±0.06	21.62±0.03	21.36±0.16	19.4±0.09	-	18.35±0.22	-	-
04:10:34.56	-48:56:32.6	10.0	23.04±0.08	21.51±0.04	21.32±0.21	19.36±0.08	-	18.26±0.18	-	-
04:10:49.88	-49:38:02.2	10.0	21.64±0.02	20.11±0.01	19.7±0.04	17.95±0.03	17.29±0.04	16.92±0.05	16.63±0.05	16.24±0.11
04:11:09.03	-49:21:51.3	12.0	23.19±0.07	21.61±0.03	21.13±0.13	19.06±0.05	-	17.95±0.13	-	-
04:11:16.74	-48:11:01.5	10.0	22.48±0.04	21.15±0.02	20.51±0.09	18.77±0.05	-	17.82±0.12	17.84±0.12	16.73±0.16
04:11:24.34	-47:31:13.8	10.0	21.94±0.03	20.4±0.01	19.98±0.06	18.15±0.03	-	17.1±0.07	16.79±0.06	16.43±0.12
04:11:50.86	-48:13:13.7	10.0	22.61±0.06	21.17±0.03	21.01±0.14	18.97±0.06	-	18.08±0.16	17.36±0.08	17.2±0.23
04:12:10.69	-45:51:34.7	12.0	22.44±0.05	20.85±0.03	20.48±0.11	18.41±0.03	17.7±0.04	17.22±0.06	-	-
04:12:15.98	-45:55:47.5	13.0	23.62±0.12	21.86±0.05	21.34±0.15	19.61±0.09	19.02±0.12	18.97±0.31	17.24±0.08	16.95±0.21
04:12:19.78	-45:50:38.8	10.0	23.08±0.08	21.5±0.03	21.07±0.14	19.38±0.07	18.79±0.09	18.42±0.19	-	-
04:13:07.29	-49:14:55.5	10.0	21.93±0.02	20.48±0.01	20.12±0.06	18.35±0.04	-	17.29±0.1	16.98±0.06	16.42±0.12
04:13:14.15	-48:29:51.0	10.0	23.05±0.06	21.58±0.03	20.97±0.12	19.23±0.09	-	-	17.77±0.11	17.95
04:13:31.27	-46:19:21.5	10.0	22.35±0.03	20.85±0.02	20.5±0.07	18.63±0.04	18.06±0.05	17.54±0.08	17.28±0.08	16.86±0.19
04:13:40.31	-49:40:56.1	12.0	22.4±0.05	21.03±0.02	20.71±0.1	18.57±0.07	17.82±0.07	17.16±0.07	16.64±0.05	16.32±0.11
04:14:14.45	-49:25:48.2	10.0	23.07±0.07	21.69±0.03	21.27±0.14	19.47±0.11	-	-	18.02±0.13	17.99
04:14:34.09	-48:59:38.6	11.0	22.79±0.05	21.33±0.02	20.96±0.1	19.29±0.09	-	-	17.33±0.08	16.51±0.13
04:14:40.26	-47:59:01.3	11.0	23.45±0.13	21.64±0.04	21.4±0.19	19.23±0.08	-	18.16±0.18	17.84±0.11	17.53±0.31
04:14:49.32	-48:04:08.0	12.0	22.91±0.08	21.41±0.03	20.71±0.15	18.9±0.06	-	17.57±0.1	17.07±0.06	16.78±0.16
04:14:49.44	-49:26:08.9	11.0	22.98±0.06	21.4±0.02	20.9±0.1	19.01±0.08	-	18.11±0.21	-	-
04:14:52.37	-49:31:48.4	11.0	22.85±0.06	21.25±0.02	20.89±0.1	18.81±0.07	-	17.77±0.15	17.52±0.09	16.9±0.17
04:15:22.48	-47:55:05.8	14.0	22.09±0.03	20.51±0.01	20.08±0.04	17.74±0.02	-	16.02±0.03	15.47±0.03	15.19±0.05
04:15:23.65	-45:58:38.4	10.0	20.79±0.01	19.26±0.01	18.78±0.02	16.97±0.01	16.29±0.01	15.8±0.02	15.51±0.03	15.33±0.06
04:15:30.35	-48:47:16.1	11.0	23.62±0.13	21.94±0.04	21.71±0.2	19.52±0.11	-	-	18.0±0.13	17.98
04:15:38.54	-47:08:26.1	10.0	23.04±0.07	21.57±0.03	21.34±0.14	19.43±0.1	-	18.59±0.27	17.88±0.12	18.11
04:16:05.51	-47:00:30.6	10.0	23.25±0.08	21.85±0.04	21.52±0.21	19.77±0.14	-	18.65±0.29	18.0±0.14	18.03
04:16:09.03	-48:01:41.9	12.0	23.15±0.09	21.58±0.03	21.17±0.13	19.08±0.07	-	17.93±0.14	-	-
04:17:53.30	-46:09:28.1	13.0	22.28±0.03	20.4±0.01	19.87±0.05	17.82±0.04	17.22±0.04	16.8±0.05	16.11±0.04	15.72±0.08
04:18:35.63	-48:21:14.1	10.0	23.02±0.08	21.5±0.03	20.97±0.11	19.23±0.05	-	18.19±0.15	-	-
04:18:43.02	-47:13:57.9	10.0	22.38±0.03	20.95±0.02	20.74±0.09	18.98±0.07	-	17.93±0.14	17.17±0.08	17.28±0.27
04:18:48.06	-46:50:02.1	10.0	22.56±0.04	21.07±0.02	20.71±0.09	18.97±0.07	-	17.72±0.12	17.58±0.11	17.16±0.27
04:19:41.67	-48:01:57.9	11.0	22.58±0.04	21.04±0.02	20.72±0.08	18.87±0.06	-	17.76±0.12	17.1±0.07	16.61±0.16
04:19:59.92	-46:59:56.2	10.0	21.57±0.02	20.02±0.01	19.66±0.04	17.75±0.02	-	16.68±0.05	16.52±0.05	16.3±0.12
04:20:08.54	-47:02:59.8	11.0	23.48±0.14	21.62±0.05	21.32±0.18	19.28±0.09	-	18.16±0.17	-	-
04:20:26.61	-48:01:37.0	14.0	23.35±0.1	21.95±0.04	21.31±0.13	19.28±0.09	-	17.73±0.12	17.06±0.07	17.01±0.23
04:21:22.62	-46:46:25.0	11.0	21.44±0.02	19.94±0.01	19.53±0.04	17.45±0.02	-	16.27±0.03	15.92±0.04	15.56±0.07
04:21:33.72	-48:11:53.6	10.0	22.19±0.03	20.67±0.01	20.32±0.07	18.43±0.03	-	17.27±0.06	-	-
04:21:38.13	-47:44:51.8	10.0	18.83±0.0	17.32±0.0	16.86±0.0	15.07±0.0	-	13.99±0.0	13.61±0.02	13.31±0.02
04:21:41.72	-48:00:33.1	10.0	23.37±0.11	21.99±0.05	21.62±0.18	19.82±0.15	-	18.71±0.28	-	-
04:21:44.61	-47:58:35.2	14.0	22.61±0.04	21.16±0.02	20.67±0.08	18.44±0.04	-	16.98±0.06	16.18±0.04	16.05±0.09
04:22:00.22	-48:06:52.1	11.0	23.1±0.09	21.57±0.04	21.31±0.2	19.31±0.06	-	17.94±0.12	17.71±0.11	17.64
04:23:43.56	-47:42:06.1	10.0	22.94±0.07	21.29±0.03	20.98±0.11	18.88±0.04	-	17.89±0.11	17.8±0.12	17.92
04:24:04.27	-47:47:37.2	10.0	22.19±0.04	20.69±0.02	20.28±0.1	18.45±0.03	-	17.32±0.07	17.01±0.06	16.65±0.15
04:24:53.10	-47:35:31.7	11.0	23.55±0.15	21.84±0.06	21.38±0.17	19.64±0.08	-	18.67±0.23	17.82±0.12	17.82

**Note:** Objects are listed in the order of RA value. The coordinates are from the DES. The object with bold coordinates is the one selected for the spectroscopy observation.

Table C.3. Two T-type UCD candidates as photometric standards in the EDF South and their photometry measurements.

$\alpha$ (hms.ss)	$\delta$ (dms.s)	SpT.	$i$	$z$	$Y$	$J$	$H$	$K_s$	W1	W2
<b>03:52:31.83</b>	<b>-49:10:59.4</b>	27.0	23.78±0.21	21.53±0.04	20.28±0.08	17.82±0.04	18.23±0.12	18.19±0.17	17.88±0.14	15.3±0.06
<b>03:59:09.81</b>	<b>-47:40:57.1</b>	28.0	-	21.82±0.03	20.59±0.06	18.06±0.03	18.3±0.06	18.53±0.19	16.87±0.06	15.19±0.05

**Note:** Objects are listed in the order of RA value. The coordinates are from the DES. SpT indicates the spectral type beginning with T0.0 as 20.0. The object with bold coordinates is the one selected for the spectroscopy observation.